EVALUATION OF COUPLING MECHANISMS IN WOOD PLASTIC COMPOSITES

By

ERICA FAY RUDE

A thesis submitted in partial fulfillment of
the requirements for the degree of

MASTERS OF SCIENCE IN MATERIALS SCIENCE AND ENGINEERING

WASHINGTON STATE UNIVERSITY
Department of Mechanical and Materials Engineering

MAY 2007

To the Faculty of Washington State University:

The members of the Committee appointed to examine the thesis of ERICA FAY RUDE find it satisfactory and recommend that it be accepted.

_____
Chair

_____

_____

ACKNOWLEDGEMENTS

First, I would like to thank Scott Hacker and Honeywell for providing the labeled MAPP to make this research possible. Second, I would like to thank my committee. Marie for all of her help and support during my time at WMEL, Armando for introducing me to Marie and all your help with wood chemistry, and Alex for all of your guidance. To all of my group members: Thank you for all of your help, time and support. I will miss you all.

To my family who have supported me through everything. You were there for me though my bachelors and supported me through my masters. You were so patient and wonderful. I love you.

To my friends who were there for those late night writing sessions, the frustrations and the celebrations, I'll never forget you.

Scott Hacker and Honeywell for supplying the labeled polymers, without those this would not have been possible.

The WSU NMR Center equipment was supported by NIH grants RR0631401 and RR12948, NSF grants CHE-9115282 and DBI-9604689 and the Murdock Charitable Trust.

This work was sponsored by the Office of Naval Research, under the direction of Mr. Ignacio Perez, under Grant N00014-03-1-0949.

EVALUATION OF COUPLING MECHANISMS IN WOOD PLASTIC COMPOSITES

Abstract

by Erica Rude, MS.
Washington State University
May 2007

Chair: Marie Pierre G. Laborie

The major components of wood plastic composites (WPCs) are wood polymers, thermoplastics, coupling agents, and lubricants. Coupling agents are used to increase the adhesion between the thermoplastic matrix and the wood, thus increasing the mechanical properties, while lubricants increase the speed of production and surface properties. Maleic anhydride polypropylene (MAPP) is a commonly used coupling agent in WPCs, while ethylene bisstearamide (EBS), the ester based Optipak 100 (OP100) and zinc stearate (ZnSt) are widely used lubricants. WPCs containing both MAPP and EBS or OP100 show no significant decreases in mechanical properties, while those containing ZnSt have a marked decrease. Currently the chemical interactions between wood and MAPP, and lubricants and MAPP are not well understood. This study focused on the chemical interactions between MAPP and wood polymers, MAPP and lubricants, and ternary blends of MAPP, wood polymers, and lubricants. Solid state ^{13}C cross polarization magic angle spinning nuclear magnetic resonance (^{13}C CP MAS NMR) spectroscopy and Fourier transform infrared (FTIR) spectroscopy were employed to determine the mechanism behind the coupling of MAPP with wood and how these interactions may be hindered by ZnSt. Initially the interaction between MAPP and cellulose, lignin and maple was examined to determine how MAPP interacts with these to produce higher mechanical properties.

Evidence of esterification and hydrogen bonding between MAPP and cellulose, lignin, and maple was uncovered. Secondly the interaction between MAPP and EBS, OP100, and ZnSt was examined to determine what, if any interactions were present. EBS and OP100 had no covalent interactions, while strong evidence of hydrogen bonding between these lubricants and MAPP was uncovered. The ZnSt/MAPP blend had significant anhydride bonding between the MAPP and the stearate groups. Zinc disassociates from the stearate groups leaving the free stearic acid groups to bond with the MA moieties of the MAPP. This warranted the study of ternary blends to determine if the MAPP/wood polymer interaction or the MAPP/ZnSt interaction would be favored. These studies showed significant favoring of the MAPP/ZnSt interaction over that of the MAPP/wood polymer interactions. The ZnSt successfully inhibits the ability of MAPP to effectively couple with wood, thus decreasing the efficacy of MAPP as a coupling agent.

TABLE OF CONTENTS

List of Figures

List of Tables

List of Equations

Chapter 1 Introduction

1.1 Introduction

In recent years a new class of structural composites have been developed. Wood plastic composites (WPCs) contain wood (e.g. maple, pine) or wood polymers (e.g. cellulose, lignin), and thermoplastics, such as polypropylene and polyethylene. This new class of composites is advantageous as it incorporates the low density, low cost, UV resistance, high specific strength and modulus, renewability, and machining properties of wood while the thermoplastic acts as a barrier to natural degradation, provided there is good adhesion between the wood and thermoplastic (Kazayawoko, 1999; Harper, 2004; Jana, 2002; Matías, 2000). It has been noted that the polar wood and the non-polar thermoplastic to not readily interact (Lu, 2000; Matías, 2000). This leads to poor stress transfer at the interfaces, opening channels for moisture and biological attack on the wood (Harper, 2004; Kazayawoko, 1999). A large amount of research has been devoted to improving the interfacial adhesion between the wood and the thermoplastic.

Chemical methods have been widely studied as a method of improving adhesion. These methods include using a third component to modify the surfaces of one or both components to enhance the adhesion. This can be done during mixing, before mixing, or adding the component directly to the mixture for melt processing (Lu, 2000). The third component is referred to as a compatibilizer or coupling agent, and for the purpose of this study will be referred to from here on as a coupling agent. Various chemicals have been used in literature as possible coupling agents. These include maleic anhydride (MA), maleic anhydride polypropylene, (MAPP), maleic anhydride polyethylene (MAPE), isocyanates, silanes, as well as other anhydrides such as acetic and succinic anhydride. Monomers can be grafted onto wood fibers or onto a thermoplastic matrix; e.g. MAPP or MAPE (Lu, 2000). The most common example of a

coupling agent is the MAPP copolymer, which has gained attention due to the increase in tensile and flexural strengths of PP based wood plastic composites, WPCs (Wolcott, 2000). Current literature cites esterification and the formation of an adhesive bridge between the components (Kazayawoko, 1999; Lu, 2005; Hristov, 2003). MAPP is very effective at low concentrations when dry blended with natural fibers and PP. Dry blending of MAPP, at 2-8% (Lu, 2000), is a very cost effective method as it can be purchased commercially and does not require any pretreatment of the fibers or polypropylene matrix before processing (Harper, 2004). Coupling agents, including MAPP, are suggested to interact with the wood by either covalent bonding or strong secondary interactions, e.g. hydrogen bonding (Wang, 2003). The possibility of co-crystallization or chain entanglement between the MAPP and the PP is also thought to be a cause for the increased mechanical properties seen when MAPP is used as a coupling agent in PP based WPCs (Harper, 2006; Lu, 2005; Felix, 1993).

Wood plastic composites also contain several other additives, including talc (0-25%), thermosets, lubricants, stabilizers and plasticizers in small amounts, 2-3%. Lubricants are used in order to enhance the ability of the components to pass into and then through the extruders unhindered as well as lead to a smoother and more desirable surface. Ethylene bisstearamine (EBS), the polyester OptiPak 100 (OP100), and zinc stearate (ZnSt) are among the most common lubricants. Lubricants can be used either alone or in blends such as a 2-1 of ZnSt and EBS (Harper, 2004). It has been proven in some cases that the addition of certain lubricants decreases the mechanical properties of the composite. Substantial gains in MOR, modulus of rupture, and MOE, modulus of elasticity, seen in MAPP containing WPCs, are significantly decreased when ZnSt is used as a lubricant. Several reasons for this include the poor distribution of the wood fibers, migration of the lubricant to the wood plastic interface, a change in morphology of the

plastic and chemical reactions between the lubricant and the coupling agent (Harper 2006). Current literature has shown that the incorporation of certain lubricants such as zinc stearate, will negate the effectiveness of the MAPP (Harper, 2004). It was found that competition from certain lubricants restricts coupling agent access to the surface of wood fibers and alters the crystallization kinetics of the polymer matrix (Wolcott 2000). This indicates that the chemical interactions as well as the morphology and phase separation of the composite are important in the enhancement of mechanical properties of wood plastic composites.

Both coupling agents and lubricants play an important role in the mechanical properties of wood plastic composites. In order to understand the reasons behind the behavior seen the chemical interactions between MAPP and wood fibers as well as lubricants further study into these interactions is needed. To date it has been shown via FTIR spectroscopy that esterification has been observed between MAPP and cellulose but not between MAPP and lignin or wood flour. FTIR spectroscopy has also shown that there is a significant interaction between MAPP and ZnSt, though, it is not yet fully understood. The goal of this study is to gain a better understanding of the interaction between the MAPP and wood, between MAPP and lubricants, and which reactions are favored in a system containing all three components.

In order to do this both attenuated total reflectance Fourier transform infrared (ATR-FTIR)spectroscopy and solid state ^{13}C cross polarization magic angle spinning nuclear magnetic resonance (^{13}C CP MAS NMR) spectroscopy will be employed. FTIR spectroscopy has been used in many studies to study coupling agents, specifically MAPP and wood (Kazayawoko, 1999) and to some extent WPCs containing MAPP, wood and lubricants (Harper, 2004, 2006). Solid state ^{13}C CP MAS NMR spectroscopy will be useful in this study as it is used to identify different chemical bonds and functional groups as well as how these groups interact

with each other. Structural and morphological information can be obtained from solid state NMR spectroscopy and this will be helpful in determining the interactions taking place within wood plastic composites.

This thesis will be divided into two major studies. Chapter two will review the interactions between MAPP and cellulose, lignin, and maple. This chapter will determine how MAPP is interacting with wood whether it be via primary interactions such as covalent bonding or through secondary interactions such as hydrogen bonding. Both NMR spectroscopy and FTIR spectroscopy will be used to determine and detail these interactions.

Chapter three with involve the determination of the interactions between popular lubricants, ZnSt, EBS and OP100 with MAPP. Based on the results ternary blends will be made in order to find which interactions are favored, whether it be between the MAPP and lubricants, or MAPP and wood, which is the intended use of the coupling agent.

In conclusion Chapter four will review the results of the aforementioned studies as well as suggestions for future work and successful blends of coupling agents, wood polymers and lubricants.

1.2 References

Felix JM, Gatenholm P. 1993. Formation of entanglements at brushlike interfaces in cellulose-polymer composites. Journal of Applied Polymer Science, 50: 699-708.

Hristov V, Vasileva S. 2003. Dynamic mechanical and thermal properties of modified poly(propylene) wood fiber composites. Macromolecular Materials Engineering, 288: 798-806

Harper D, Wolcott M. 2004. Interaction between coupling agents and lubricants in wood-polypropylene composites. Composites Part A, 35: 385-394.

Harper DP, Wolcott MP. 2006. Chemical imagining of wood-polypropylene composites. Applied Spectroscopy, 60: 898-905.

Kazayawoko M., Balatinecz JJ, Matuana LM. 1999. Surface modification and adhesion mechanisms in woodfiber-polypropylene composites. Journal of Materials Science, 34: 6189-6199.

Jana SC, Priet A. 2002. Natural fiber composites of high-temperature thermoplastic polymers: effects of coupling agents. Journal of Applied Polymer Science, 86: 2168-2173.

Lu JZ, Wu Q, McNabb HS Jr. 2000. Chemical coupling in wood fiber and polymer composites: a review of coupling agents and treatments. Wood and Fiber Science, 32: 88-104.

Lu JZ, Wu Q, Negulescu II. 2005. Wood-fiber/high-density-polyethylene composites: Coupling agent performance. Journal of Applied Polymer Science, 96: 93-102.

Lu JZ, Negulescu II, Wu Q. 2005. Maleated wood-fiber/high-density-polyethylene composites: Coupling mechanisms and interfacial characterization. Composite Interfaces, 12: 125-140.

Matías MC, De La Orden MU, Sánchez CG, Urreaga JM. 2000. Comparative spectroscopic study of the modification of cellulosic materials with different coupling agents. Journal of Applied Polymer Science, 75: 256-266.

Wang Y, Yeh FC, Lai SM, Chan HC, Shen HF. 2003. Effectiveness of functionalized polyolefins as compatibilizers for polyethylene/wood flour composites. Polymer Engineering and Science, 43: 933-945.

Wolcott M, Chowdhury M, Harper D, Li T, Heath R, Rials T. 2000. Coupling agent/lubricant interactions in commercial wood plastic formulations. The Sixth International Conference on Woodfiber-Plastic Composites, 197-204.

Chapter 2 Evaluation of Interactions between MAPP and Wood Polymers

2.1 Abstract

The major components of wood plastic composites (WPCs) are wood polymers, thermoplastics, coupling agents, and lubricants. Maleic anhydride polypropylene (MAPP) is a commonly used coupling agent in polypropylene based WPCs. It has been noted in practice that the use of MAPP significantly increases the mechanical properties in PP based WPCs, although the mechanism leading to this improvement is only partially understood. Most research has been done on the interaction between MAPP and cellulose, as cellulose is a major component of wood. The current knowledge base suggests that esterification and hydrogen bonding occurs between MAPP and cellulose. In order to further the knowledge base on the interaction between MAPP and wood the chemical interactions between MAPP and wood polymers were studied with solid state ^{13}C CP MAS NMR spectroscopy and FTIR spectroscopy, to determine the mechanism behind the coupling of MAPP with wood. In order to use NMR spectroscopy, ^{13}C labeled MAPP was required to enhance the visibility of the maleic anhydride groups. Esterification was seen between MAPP and cellulose by not only FTIR spectroscopy, but clear indications of this reaction was seen in the NMR spectrum. Some evidence of hydrogen bonding was also seen between the maleic anhydride functional groups and the cellulose. A lignin and MAPP blend was also studied and it was clearly evident in the NMR spectra that there was esterification and hydrogen bonding between the MAPP and the lignin. This has yet to be seen in other research as with MAPP and lignin there is a large overlap between the functional groups of lignin and ^{12}C MAPP in an FITR spectrum. Using labeled MAPP the bands were separated at a new band was seen at 1637cm^{-1}, indicating the presence of an ester bond. Finally maple was

compounded with MAPP and again it was apparent that esterification was occurring between the MAPP and the maple. The new band seen in lignin at 1637cm^{-1} was also seen in the maple/MAPP blend. This was again indication that esterification was occurring and not only between cellulose but also between lignin and MAPP.

2.2 Introduction

In recent years the interest in wood plastic composites has increased significantly (Deligio, 2006). Due to the poor interactions between the hydrophilic wood and the hydrophobic polyolefin there is inadequate adhesion between the wood and plastic. Considerable research has been performed to improve interfacial adhesion; one method of this includes adding a coupling agent into the composite. Maleic anhydride polypropylene (MAPP) is a widely used coupling agent within polypropylene based composites. The addition of MAPP shows a marked increase in the modulus of rigidity, MOR, and modulus of elasticity, MOE, of polypropylene, PP, based composites, indicating some form of interaction between the matrix and the MAPP (Wolcott, 2000, .

MAPP exists in two forms, an anhydride and an di-carboxylic acid form. Heinen et al determined the most probable structure of MAPP (Figure 2.1) using smaller model compounds studied in solution with ^{13}C NMR spectroscopy (Heinen, 1999). This structure contains the anhydride form of MA grafted on the PP backbone. The current hypothesis states that MA functional groups are capable of chemically bonding with wood, via ester bonds or secondary interactions such as H-bond (Figure 2.1), while the PP backbone of MAPP may entangle and recently co-crystallize with the rest of the PP matrix (Figure 2.2) (Bratawinjaja, 1989; Takase, 1989; Sanadi, 1992; Harper 2006).

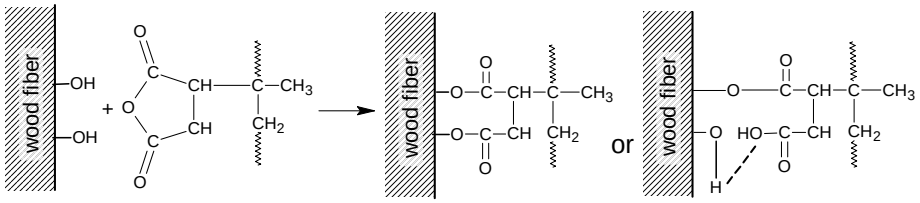

Figure 2.1 Reaction Schema of MAPP and wood fibers (Takase, 1989)

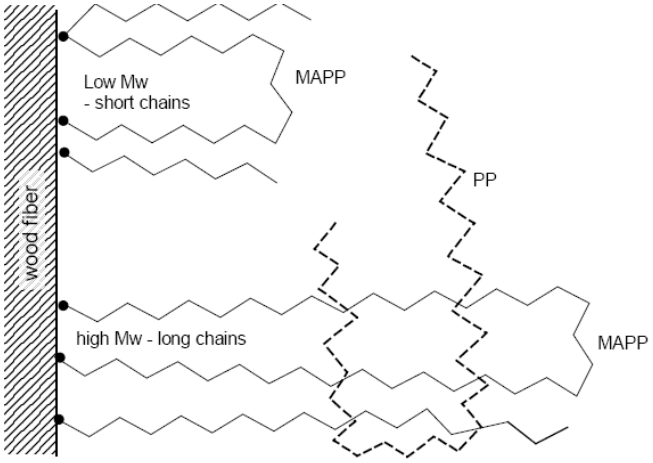

Figure 2.2 MAPP/PP polymer entanglement and/ or co-crystallization (Sanadi, 1992)

Current research in the chemical interactions between MAPP and cellulose suggests esterification as the main interaction with a possibility of hydrogen bonding (Figure 2.1) as well (Takase, 1989, Carlborn and Matuana, 2006). Avella et al proposed that MA groups migrate towards the fiber surface due to the polar/non-polar interactions, thus increasing the probability of bonding between the MA and the hydroxyl groups on the wood fibers or cellulose (Avella, 1998).

Using IR spectroscopy, several researchers have confirmed the existence of ester bonds between cellulose fibers and MAPP when the polymer blend has been prepared by solution casting (Felix, 1991; Joly, 1996). The symmetric stretching band of MA sits between 1792 and 1787 cm^{-1}, while an ester band would be seen at 1722-1746cm^{-1}(Qui, 2006). Kazayawoko et al have shown that ester links are formed between cellulose and MAPP as well as between bleach

kraft pulp (BKP) and MAPP, while there is no evidence of esterification between thermomechanical pulp (TMP) and MAPP (Kazayawoko, 1997; Kazayawoko, 1999). The TMP, BKP and the cellulose were reacted with MAPP in a solution of xylene and reacted for 2 hours between 130-140˚C. Felix et al immersed cellulose fibers in a solution of 5 wt % MAPP on the fibers and toluene at 100˚C for 5 minutes and then Sohxlet extracted for 48hrs to remove any non-covalently bonded components from the fibers (Felix, 1991). The fibers were then dried to a constant weight. FTIR spectroscopy of the cellulose/MAPP fibers showed MAPP was covalently bonded to the cellulose fibers via esterification. Matías et al used the same procedure to treat cellulosic materials with MAPP as Felix et al, although the MAPP was pretreated by heating at 160˚C for 5 minutes to create a larger amount of the more reactive anhydride complex via the elimination of water (Matías, 2000; Felix, 1991). The MAPP treated cellulose was determined via FTIR spectroscopy to have new ester bonds forming after treatment, as seen by the absorption band at 1730 cm^{-1}.

The interactions between MAPP and cellulose after melt mixing have also been studied (Qui, 2004; Qui, 2004, Qui, 2006). This sample preparation is more relevant to extrusion processes. Both melt mixing and ball mixing were performed and it was determined that the mechanochemical formation of reactive OH groups on the cellulose was the primary factor in the esterification between MAPP and cellulose. The symmetric stretching band of the MA sits between 1792 and 1787 cm^{-1}. The FTIR data showed a new band characteristic of an ester at 1730 cm^{-1}, thus indicating esterification. No difference in esterification was seen when different MAPP structures were used. It was also determined that ball-milling produced more esterification in the mix than melt-mixing due to the mechanochemical activation, leading to higher interfacial adhesion. When even small amounts of MAPP are used enhanced interfacial

adhesion, MOR and MOE, is achieved, even though the FTIR spectra does not show the presence of ester bonds. This could be due to the low number of ester bonds due to low amounts of MAPP. The increased interfacial adhesion is still attributed to an esterification reaction between MAPP and cellulose (Qui, 2005), although other mechanisms may contribute to the enhanced interfacial adhesion. As a conclusion, while there is strong evidence for esterification between MAPP and cellulose; no evidence has been found to show esterification between wood or lignin and MAPP. An additional spectroscopic technique would be useful to further probe interactions between MAPP and wood constituents.

Solid State ^{13}C NMR spectroscopy has been particularly useful for the study of solid phase polymers as it gives detailed information of the types of functional groups present through the chemical shifts seen in the resulting spectrum, as well as morphological information (Parker et al, 1989). Each carbon has a distinctive chemical shift defined by its unique electronic environment. If a change in chemistry, such as new bonds, occurs a change in chemical shift may be seen. Another possible sign of new bonds or a change in the ratio of species present is a change in the peak shape or intensity. Furthermore, the intimacy between polymer phases or nanoscale morphology in polymer blends can be determined via relaxation time measurements, such as proton spin lattice relaxation in the rotating frame $^{H}T_{1\rho}$s (Silva et al, 2000). Upon blending two polymers, a change in $^{H}T_{1\rho}$ in the individual polymers, would indicate a change in the molecular motion of the polymer that could be due to molecular interactions.

In addition, in polymer blends similar $^{H}T_{1\rho}$s as measured through carbons pertaining to each of the polymer, indicates either a similar motional regime or homogeneity on a nanoscale level induced by spin diffusion. Therefore altogether $^{H}T_{1\rho}$ measurements would be another

insightful way to probe intimacy and interactions between MAPP and wood polymers by solid state NMR spectroscopy.

To determine $^{H}T_{1\rho}$ associated with each carbon a variable contact time cross-polarization pulse can be used. From these experiments the intensity of each peak is plotted against the contact time. The magnetization equation below is then used to fit the resulting curve allowing for the $^{H}T_{1\rho}$ for each peak to be obtained (Schmidt-Rohr and Spiess, 1994).

Equation 2.1 Magnetization Equation

$$I(t) = I * ({}^{H}T_{1\rho} / ({}^{H}T_{1\rho} - T_{CH}))(\exp^{-t/T_{1\rho}} - \exp^{-t/T_{CH}})$$

The $^{H}T_{1\rho}$s determined for each peak can then be compared with that of the same peaks in a blend or after a reaction to determine if motional characteristics have changed.

Not only has solid state NMR spectroscopy been used to study the morphology of polymers, but it has also been used to study the structure and behavior of wood and other lignocellulosic materials, such as lignin and cellulose (Maunu, 2002 and Gil and Neto, 1999). The combination of wood and polymers to create wood plastic composites can therefore be studied via solid state NMR spectroscopy.

Currently the chemical interactions between MAPP, wood and wood polymers is still not clear. Due to the extremely useful nature of NMR spectroscopy to determine morphology of polymer blends and the ability to identify structure and behavior of wood this technique will be applied to wood plastic composites. The particular blends to be studied will include MAPP with wood and with wood polymers, cellulose and lignin. From these blends it is hoped that if there are chemical interactions occurring between MAPP and wood, as well as its derivatives, that these reactions may be visible in the solid state NMR spectroscopy experiments. The

determination of the specific interactions that may be occurring, may later aid in the development of more effective coupling agents.

2.3 Experimental

2.3.1 Materials

Solid State ^{13}C CP NMR spectroscopy only detects the ^{13}C form of carbon which is of 1% natural abundance. With even a small amount of MA grafted onto the PP backbone the detection of the MA would be very low. To increase the visibility of the MA functional group 100% ^{13}C enriched MAPP at the C1 and C4 carbons. The ^{13}C labeled MAPP was provided by Honeywell and patterned after the A-C® 950, a commercial product. The SAP (saponification number) of the final product was approximately 41.2 mg KOH/gm (3.6 wt % MA) with a viscosity of 2,200 cps @ 190 °C. (Figure 2.4). The C1 and C4 carbons were chosen because they are the functional groups that are believed to be involved in the coupling mechanisms with wood. The cellulose powder, Indulin lignin, and acer saccharum (sugar maple) were all purchased commercially.

2.3.2 Sample Preparation

The ^{13}C labeled MAPP, cellulose, lignin, and maple were dried under vacuum to a constant weight and stored under vacuum, as were the resulting heated components and the blends. To determine MAPP/wood polymer interaction three blends were made at a weight ratio of 1:1, cellulose/MAPP, lignin/MAPP, and maple/MAPP. Before the blends were processed unlabeled blends were used to remove any impurities from the injection molder. The ^{13}C labeled blends were mixed via a Dynisco Laboratory Mixing Molder (injection-molder). The samples

were processed at 180°C and 50 rpm for 2 minutes, minimizing thermal degradation of the components. These samples were then divided into three separate replicates that were deemed for CP/MAS and FTIR spectroscopic analysis. Furthermore, control samples consistent of the neat components, MAPP, cellulose, lignin, and maple, that had been heated in an oven at 180˚C for 2 minutes, were evaluated for comparison with the blends; these components will be considered neat components.

2.3.3 NMR Spectroscopy

2.3.3.1 Solution ^{13}C NMR Spectroscopy

Maleic anhydride samples prepared for solution NMR spectroscopy were prepared using a 1M solution of maleic anhydride dissolved in D_2O. To determine the chemical shift of the diacid form of the MA, a portion of the 1M solution was brought to a pH of 11 using sodium hydroxide pellets, while a second portion was brought to a pH of 1 using HCl to determine the chemical shift of the anhydride form of MA. These spectra for each solution were then run on a Varian Mercury Vx 300 with a Bruker 7.05T, 54 mm bore magnet with a Nalorac 4-nucleus Plus 5mm probe, 1H-19F-13C-31P or 1H-X where X is tunable from 30 to 150 MHz. The spectral width was from -5ppm to 220ppm with 256 scans and a recycle delay of 1sec.

2.3.3.2 CPMAS NMR Spectroscopy

All NMR spectroscopic experiments were performed on a Bruker Avance 400. A 3.50μs proton 90 degree pulse was used with different contact times for the ^{13}C and ^{1}H channels and a proton decoupling field strength of 70 kHz, spun at 5 kHz, with a recycle delay of 4 seconds, and a 22msec acquisition time. The probe used was a chemagnetics 7.5mm double resonance probe

with a 7.5mm solid state rotor with a zirconia sleeve and the cap, turbine, and spacers are Kel-F. The spectrometer was referenced using adamantane. Three replicates were analyzed by NMR spectroscopy and the chemical shifts were compared via t-test with an alpha value of 0.05. The neat components and the blends were analyzed at the optimum contact time of 1ms. The data was analyzed to determine if changes in the chemical shifts were present. Once changes were determined all neat components as well as the blends were subjected to variable contact time experiments. CP experiments with variable contact times (18 contact times, 0.025 ms to 6 ms) were run under the same parameters as the 1 ms contact time experiments. The data was then plotted and curve fit using OriginPro7 according to Eq. 1 in order to determine HT1rho of each identifiable carbon. , T-tests were used to determine significant changes ($p \leq 0.05$) in HT1rho within a system and also before and after blending. Tukey tests were also used to determine similarity between relaxation times to group the peaks, indicated by the letters A, B, C... after the reported relaxation time.

2.3.4 FTIR spectroscopy

FTIR spectroscopy is frequently used to determine the presence of ester bonds between MAPP and cellulose it was again used in this study to aid in determination of new bonds formed (Bratawinjana, Carlborn, Felix, Kazayawoko, Harper, Matís, Qui). Spectra were collected using a ThermoNicolet Avatar 370 spectrometer (Thermo Electron Corporation), in the attenuated total reflection (ATR) mode (SmartPerformer, ZnSe crystal). The absorbance spectra were mathematically ATR corrected using the Omnic 7.0 software package. Each spectrum was taken as an average of 64 scans at a resolution of 4 cm^{-1}, with three replicates of each sample.

2.4 Results and Discussion

2.4.1 MAPP Characterization

The NMR spectrum of MAPP shows two distinct peaks at 180.1ppm and 173.5ppm in the carbonyl region that arise from the ^{13}C enriched C_1 and C_4 carbons of the maleic moieties. (Figure 2.4). In addition, a shoulder at 165.6ppm appears. There are also two peaks that appear at 130ppm and 123ppm, identified by a * in the spectrum. These peaks are artifacts on the spectrum and are called spinning side bands. Spinning sidebands are spaced at the spinning frequency (in this case 5000Hz)from the isotropic shifts (180.1ppm, 173.5ppm), approximately mirror the shape of the isotropic shifts, and have a lower intensity (Macomber, 1998). To confirm the peaks at 130ppm and 123.5ppm the distance between these and the isotropic peaks was measured and determined to be 5000Hz, also the spinning speed was changed, causing these bands to shift, thus confirming they as spinning side bands. The two distinct peaks at 173.5ppm and 180.1ppm were believed to arise from the combined $C_1$and C_4 carbons of the anhydride and diacid maleic moieties, respectively. To confirm the assignment of each chemical shift to either the diacid C_1 and C_4 carbons or the anhydride C_1 and C_4 carbons, solution NMR spectra of maleic anhydride under various pH environments were acquired. Namely, maleic anhydride was dissolved in D_2O and acidified with HCl and a second solution was saponified with NaOH. The alkaline solution was expected to have the ionized diacid form of the MA while the anhydride form would be present under acidic conditions. It was determined the C_1 and C_4 carbons associated with the diacid form was present at 175.6ppm while the C_1 and C_4 carbons associated with the anhydride form appeared at 169.2ppm (Figure 2.3). From these data it was confirmed that the downfield chemical shift at 180.1ppm was the diacid carbons while the upfield shift at 173.5ppm was assigned to the anhydride form. The difference between the shifts in the solid and

liquid state is likely due to the presence of the polypropylene backbone and the difference in state (Heinen, 1999).

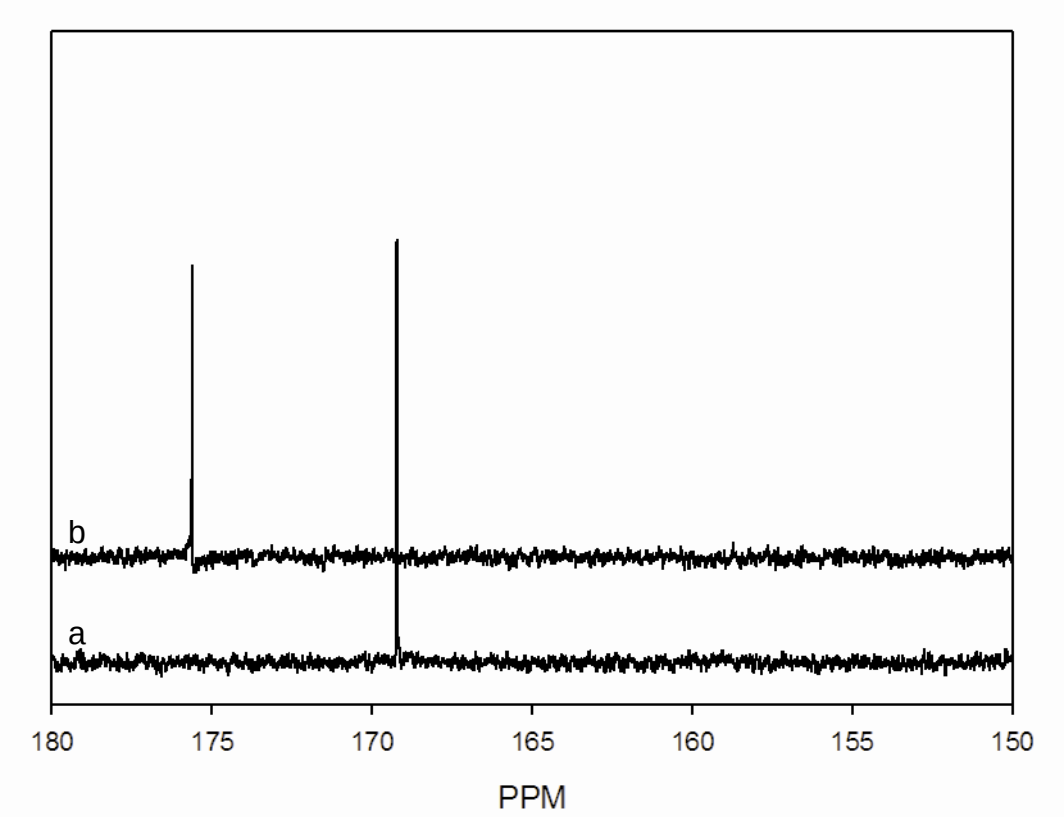

Figure 2.3 ^{13}C NMR spectra of a) anhydride form of MA at pH 1; b) diacid form of MA at pH 11

Chemical predictions using ChemDraw Ultra were made to determine the nature of the peak at 165.6ppm in the labeled ^{13}CMAPP. This peak was found to be the result of the anhydride grafted to the end of a PP chain by a double bond. Outside the carbonyl region, the main chain carbons are observed at 44.4, 26.4 and 21.9ppm. The peak at 21.9ppm corresponds to the methyl group on PP, while the peak at 26.4ppm is the tertiary carbon and the final peak at 44.4ppm is the secondary carbon, joining tertiary carbons, (Figure 2.4). Once the chemistry of MAPP was understood, its phase morphology could be evaluated by $^{H}T_{1\rho}$.

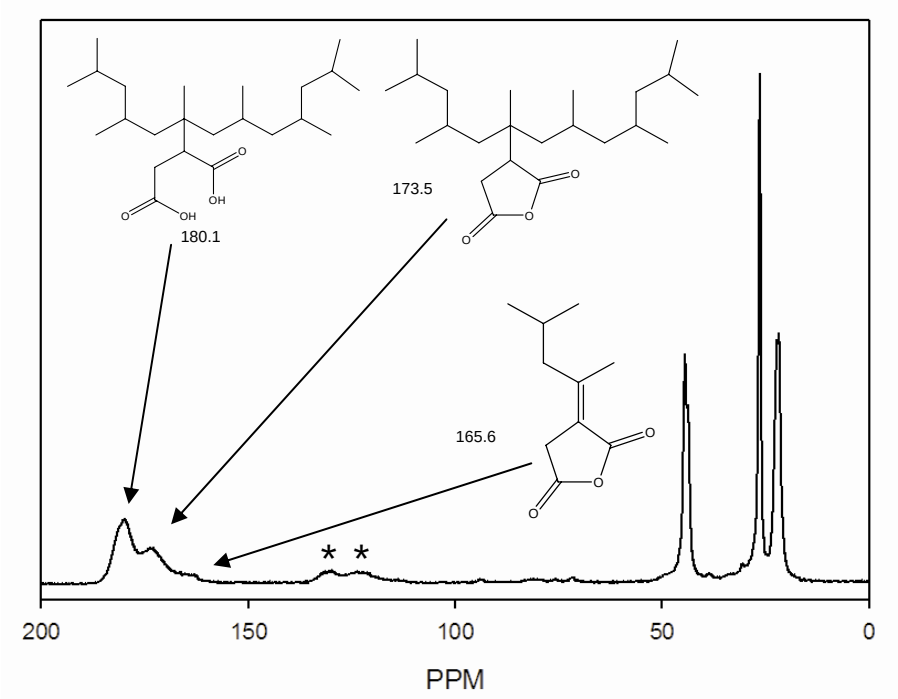

Figure 2.4 Solid State ^{13}C NMR spectra of MAPP and assigned structures

Table 2.2 contains the chemical shifts for neat ^{13}C MAPP as well as the $^{H}T_{1\rho}$ associated with each carbon. The relaxation times were grouped via the Tukey test in order to determine the level of homogeneity, and the groups are denoted A,B,C, etc. The two peaks corresponding to the functional groups of maleic anhydride have similar $^{H}T_{1\rho}$s, while the PP carbon peaks all have similar relaxation times. From this it can be concluded that the MA carbon groups have distinct molecular motion or are phase separated from the main chain PP. This type of behavior appears to reflect a structure in which the main chain PP entangles and crystallizes, excluding the MA groups from the PP structure.

As supportive data FTIR spectroscopy was employed on the neat MAPP. Again, the MAPP used for IR characterization was ^{13}C labeled, therefore a comparison to that of unlabeled MAPP was needed to first determine the exact placement of the two anhydride bands present in MAPP. Using the equation for reduced mass, the equation for the vibration frequency of a

molecule, and the ratio of this frequency for the unlabeled and ^{13}C labeled MAPP, the values for the two anhydride bands were calculated to appear at approximately 1740 cm^{-1} and 1690 cm^{-1}, while the normal ^{12}C bands would be seen at approximately 1810 cm^{-1} and 1760 cm^{-1} (Table 2.1).

Equation 2.2 Reduced Mass

$$\mu = \frac{m_1 m_2}{m_1 + m_2}$$

Equation 2.3 Vibration Frequency

$$\nu = \frac{1}{2\pi}\sqrt{\frac{k}{\mu}}$$

Table 2.1 Comparison of ^{12}C and ^{13}C vibrational frequencies

Functional Group	^{12}C* (cm^{-1})	^{13}C (cm^{-1})	^{12}C-^{13}C (cm^{-1})
Anhydride	1810, 1760	1740, 1690	1775, 1725
Ester	1735	1670	1700
Aldehyde	1725	1660	1690
Ketone	1715	1650	1680
Carboxylic acid: free/H-bonded	1760/1710	1690/1645	1725/1675
Acetate ester	1750	1680	1715

*Pavia et al, 1996

From the FTIR spectrum below, the 2 anhydride bands of the labeled ^{13}C MAPP used in this study are present at 1733 cm^{-1} and 1670 cm^{-1}. The band at 1733 cm^{-1} is the asymmetrical stretching band while the band at 1670 cm^{-1} is the symmetrical stretching band. The carboxylic band appears at 1670 cm^{-1} as well, indication that the band seen in the spectrum is a combination of both the anhydride and carboxylic bands. The shoulder seen at 1700cm^{-1} is not specifically assigned in the neat MAPP as this is a weak shoulder. In an effort to determine if esterification is present the ratio between these two bands will be compared, and an ester band will be looked for. Initially the ratio based on area of 1670/1733 is 0.98 and the ratio for intensity is 0.94, while the ratios for intensity and are for 1700/1733 are 0.69 and 0.42 respectively. As the ester band

would be a combination of a ^{12}C carbon from the cellulose, lignin, or maple, and a ^{13}C carbon from the MAPP, the ester band would be expected at approximately 1700 cm^{-1} instead of 1735 cm^{-1}, as determined by the reduced mass and the ratio of the frequency equation as used above. The use of ^{13}C MAPP may move the ester band out from under the anhydride bands, possibly leading to easier identification of new ester bonds.

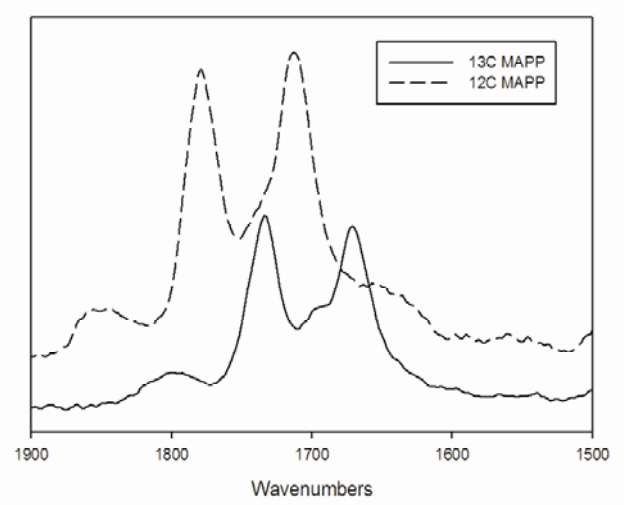

Figure 2.5 FTIR spectra of ^{12}C and ^{13}C rich MAPP

2.4.2 Cellulose/MAPP blend

The cellulose/MAPP blend was evaluated with ^{13}C CP NMR spectroscopy and the resulting spectrum was first inspected for new peaks and changes in current peaks (Figure 2.6). All chemical shift data is summarized in Table 2.2. A new peak can be seen at 32.6ppm. This peak indicates a new species that was not present in either of the two neat components before blending. The possibility of contamination from the rubbing alcohol used to clean the rotors was reviewed but ruled out based on the chemical shift assignments. Based on the position of this peak and the intensity it appears to be a methylene (CH_2) carbon. A methylene carbon at

32.6ppm could occur as a result of MAPP chain scission or PP degradation. Since the main chain carbons was not the focus of this study, no further investigations in this new chemical shift were attempted.

The next change noted is the difference in intensity of the carbonyl MA signals, at 180.1ppm and 173.5ppm. The 173.5ppm peak, is assigned to the anhydride form of MAPP, is much more pronounced in the blend, and both peaks are also much broader than in the neat ^{13}C MAPP. This intensity change is possibly due to a change in the ratio of species underlying these chemical shifts, namely the diacid versus anhydride C_1 and C_4 carbons, esterification between MAPP and cellulose, a change in their relaxation time of the peak at 173.5ppm, or hydrogen bonding. However, the relaxation times of these resonances in the neat MAPP and in cellulose/MAPP blend are the same (Table 2.3) therefore the hypothesis of a change in relaxation time can be eliminated (Schimdt-Rohr and Spiess, 1994).

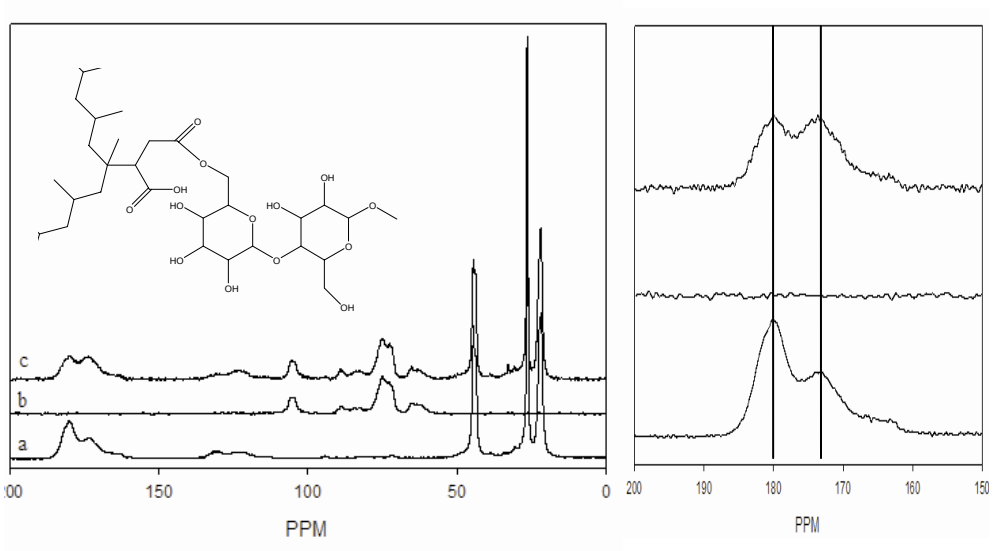

Figure 2.6 Full ^{13}C NMR spectra (left) of MAPP (a), cellulose (b) and cellulose/ MAPP (c), and close up spectrum (right) of the carbonyl region for a, b, c

A change in the acidity of the blend could cause a change in the equilibrium (Figure 2.7) between the diacid (180.1ppm) and the anhydride (173.5ppm) forms. An increase in the

anhydride form would lead to a greater intensity in the peak at 173.5ppm, as seen in the NMR spectrum of the blend (Figure 2.6). The double bond of the maleic anhydride is lost during the grafting process, therefore the resulting group resembles that of succinic anhydride. In order to determine if acidic conditions introduced by the cellulose, pH = 5.5 (Poptoshev et al, 2000), affect the equilibrium, the pKa's of succinic anhydride were used. Succinic acid is a dicarboxylic acid with pKa's of 4.16 and 5.61 (Vollhardt and Schore 1999). At a pH of 5.5, and using a pKa of 4.16 to account for both carboxyl groups, it was determined that the ratio of diacid to anhydride species is 21.9, Equation 2.4 (Vollhardt and Schore 1999). In order for more of the anhydride to form the pH would need to be below 4.16, otherwise the environment favors that of the diacid form. The spectrum of the cellulose/MAPP blend, in fact does not show an increase in the diacid form of the MAPP, 180.1ppm, indicating that the change in intensities is not due to a shift in the MAPP equilibrium.

Equation 2.4 pH

$$pH = pKa + \log([B^-]/[HB])$$

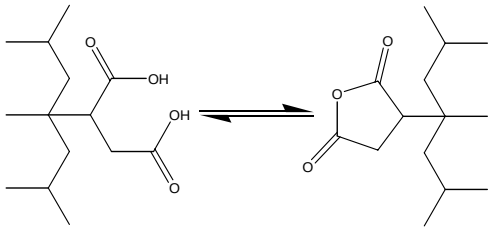

Figure 2.7 Equilibrium of the acid and anhydride forms of MAPP

The possibility of either or both carboxylic carbons C_1 and C_4 being involved in an esterification reaction with the cellulose was examined via chemical shift predictions, as well. The predicted chemical shift for an ester from the MAPP/cellulose bond is 174.5ppm with the remaining carboxyl group appearing at 177.0ppm (Figure 2.6). If esterification between

cellulose and MAPP occured, a signal at 174.5-177.0ppm is likely to be observed together with peak broadening. This phenomenon of cellulose hydroxyl groups to MAPP esterification was observed as shown in Figure 2.6. However, no observable changes in cellulose signals were observed. This is not unexpected as there is a higher proportion of cellulose hydroxyl groups relative to MA groups in the blend which may mask any subtle differences.

Table 2.2 ^{13}C NMR data for Cellulose/MAPP blend

Chemical Shifts for Cellulose/MAPP blend (ppm)					**Relaxation Time ($^{H}T_{1\rho}$, ms)**			
Peaks (ppm)	**MAPP**	**Cellulose**	**Cellulose/ MAPP**	**ppm change**	**MAPP**	**Cellulose**	**Cellulose/ MAPP**	**$^{H}T_{1\rho}$ change**
180	180.1±0.3		180.0±0.4		3.6±0.3A		3.6±0.4B	
173	173.5±0.1		173.4±0.3		3.9±0.1A		3.9±0.3AB	
105		105.6±0.1	105.3±0.4			5.5±0.4A	4.3±0.8AB	
89		89.0±0.2	89.3±0.5			6.4±0.9A		
83		83.4±0.9	82.7±0.6			5.3±0.4A		
74		74.9±0.1	74.8±0.1			5.0±0.5A	4.0±0.7AB	1.0ms
65		65.0±0.0	65.1±0.3			5.6±0.7A		
44	44.4±0.3		44.1±0.3		5.3±0.3B		4.6±0.2AB	0.7ms
32.6			32.6±0.2	New Peak			2.6±0.3	New Peak
26	26.4±0.3		26.2±0.2		5.4±0.3B		5.1±0.2A	
21	21.9±0.3		21.8±0.2		4.9±0.1B		4.3±0.2AB	0.6ms

Takase et al state that if a monoester forms the remaining carboxyl group may be able to hydrogen bond with other hydroxyl groups from the wood or cellulose in the blend. Due to the large amount of intra- and inter- molecular hydrogen bonding in cellulose a change in the chemical shifts of cellulose due to H-bonding with MAPP is unlikely to be seen. There are two possibilities for hydrogen bonding between cellulose and MAPP. The first possibility is the cellulose will donate a proton of a hydroxyl group to an oxygen of the MA carboxyl group, the second option is that the carboxyl group donates a proton to the hydroxyl group of the cellulose. The electron donated carbon produces small disturbances in the magnetic shield on the nucleus and causes a down field chemical shift as compared to the non-hydrogen bonded nuclei. The electron accepted carbon shifts upfield (Wu, 2000). As the different species in this study are

contained under the same broad peak, hydrogen bonding in which either carbon may be the donating or the electron accepting carbon, the resulting peak after esterification could also broaden due to the hydrogen bonding. As the MA moieties are able to participate in both hydrogen bonding possibilities described above the chemical shifts of the peaks, 180.1ppm and 173.5ppm, would be expected to broaden. Broadening of these peaks is seen in the NMR spectrum, and may also have some contribution from hydrogen bonding (in addition to the already established contribution from the new ester species). Overall, there is no clear evidence of hydrogen bonding, but the spectral features of the blend are consistent with the occurrence of both esterification and H bonding.

Phase morphology and molecular motions were examined by analyzing the $^{H}T_{1\rho}$ data. The new signal at 32.6ppm was not included in the analysis since it is likely a product of impurity or degradation. The relaxation times for both the neat components and the blend were grouped using letters, via the Tukey test. For cellulose (grouping A) all of the cellulose carbons have similar relaxation times indicating that the carbons are homogeneous. Neat MAPP on the other hand has two separate domains (A, B); one containing the maleic anhydride functional groups and one containing the polypropylene backbone. Upon blending changes in $^{H}T_{1\rho}$ can be seen in the C_2, C_3, and C_5 carbons of cellulose, at 74.9ppm, as well as the 2˚ and methyl carbons of the MAPP. These changes allow for all of the carbons in particular the MA moieties and cellulose carbons to have the same $^{H}T_{1\rho}$. This indicates that these carbons either have similar motional characteristics or that spin diffusion occurs between these carbons averaging out motional characteristics. Therefore, the changes seen allow for the MAPP carbons to be intimately meshed with the cellulose carbons. The relaxation data also shows that there is no segregation between the maleic anhydride groups, the polypropylene backbone and the cellulose.

The relaxation times are very similar and while two groups may be present (A, B) they are well overlapped and there is a large amount of meshing and homogeneity within the blend.

Based on the chemistry of MAPP the anhydride form is much more reactive than its diester counterpart (Matías, 2000). In the presence of heat and an acidic environment this reactive anhydride can esterify, causing the equilibrium of the diacid/anhydride of the MAPP would shift towards the anhydride form if the anhydride were to be consumed by a competing reaction. The increased reactivity of the anhydride over the diacid leads to the formation of monoester bonds between the cellulose and MAPP. This would occur via a nucleophilic ring opening reaction between the OH groups on the cellulose and the anhydride of the MAPP (Vollhardt and Schore 1999). It is unlikely that a diester bond forms between the cellulose and the MAPP due to steric hindrance, leaving the remaining carboxyl group the possibility of hydrogen bonding (Takase and Shiraishi, 1989). The pH of 5.5 introduced by cellulose leads to a ratio of 21.9 between diacid and anhydride forms. This indicates that the resulting ^{13}C NMR spectrum would still have a high intensity peak at 180.1ppm. This behavior was not seen and it can be therefore concluded the acidity of the cellulose was insufficient to cause any spectral changes. The decrease in intensity of the diacid peak at 180ppm with an increase in the intensity of the peak at 173ppm indicates that esterification was likely occurring, while hydrogen bonding appears to be evident due to the broadening of the peaks. The chemical shift predictions for esterification between MAPP and cellulose were also supported by the changes seen in the intensity of both the diacid and the ester peak. Overall, it can be concluded via NMR spectroscopy that esterification between cellulose and MAPP occurred during blending.

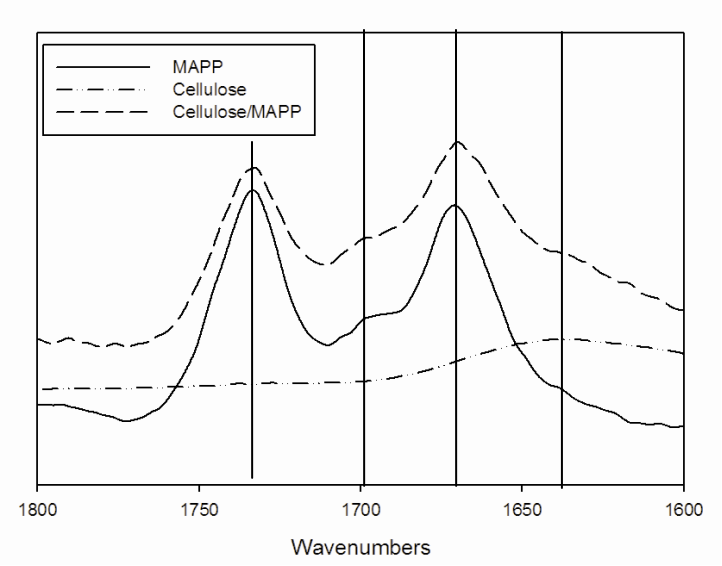

Figure 2.8 FTIR spectra of MAPP, cellulose, and cellulose/MAPP blend

Table 2.3 FTIR bands and ratios* for Cellulose/MAPP blend

Band (cm^{-1})	Band Type	Cellulose/MAPP Intensity/Area	MAPP Intensity/Area
1733	asymmetric anhydride stretch	1.00	1.00
1698	non H-bonded carboxylic acids cellulose/MAPP ester bonds	0.69(±0.03) / 0.42(±0.04)	0.52(±0.05) / 0.30(±0.04)
1670	symmetric anhydride stretch carboxylic acid stretch	1.11(±0.02) / 1.83(±0.04)	0.94(±0.01) / 0.98(±0.04)

*ratios normalized to area and intensity of 1733cm^{-1}

The cellulose/MAPP blend was also analyzed by FTIR spectroscopy as previously described. The resulting spectrum and the MAPP spectrum were normalized to that of the MAPP C-H stretching band at 2950cm^{-1} to allow for a comparison of intensities between the MA functional groups in the blend and the neat MAPP. The cellulose spectrum was not normalized as the C-H stretching band of MAPP was absent. From this spectrum (Figure 2.8) it can be seen that there is a small overlap of a broad cellulose band (1638cm^{-1}) near the anhydride and carboxylic acid band located at 1670cm^{-1} in the blend (Table 2.3). In the blend the band at 1671cm^{-1} appears to shift 1cm^{-1} to 1670cm^{-1}, this shift is not taken into account as the resolution of the instrument is 4cm^{-1}. It can be noted that while the intensity of the carboxylic

acid/anhydride band does not change the intensity of the asymmetrical stretching band of the anhydride at 1733cm^{-1} in the blend is much less intense than that seen in the neat MAPP. On the other hand, the anhydride-carboxylic band at 1670 cm^{-1} did change. This suggests that a decrease in anhydride may be compensated by an increase in acid signal. The ratios for 1698/1733 for intensity and area are 0.69 and .042 respectively. These ratios are higher than that of MAPP (0.52 and 0.30) and indicate that there is a presence of ester bonds, supported by the fact that the MAPP was labeled with ^{13}C and an ester bond between ^{12}C and ^{13}C carbons would lead to a band located at 1700 cm^{-1}. Also, the ratios for intensity and area for 1670/1733 are 1.11 and 1.83 respectively, higher than in MAPP alone. These increase in the ratio suggests that there is a larger amount of carboxylic acid present as the asymmetric anhydride band decreases and the symmetric anhydride/carboxylic acid band increases. This is consistent with esterification on one of the carboxylic acid groups of MAPP.

It has been suggested that hydrogen bonding may occur between the remaining carboxyl group and the monoester and would be seen at 1739cm^{-1} for unlabeled MAPP. This translates a range of approximately 1700-1710cm^{-1} for ^{13}C labeled MAPP, which overlaps with the already present anhydride and carboxylic bands, therefore the presence of hydrogen bonding is inconclusive. The hydroxyl region of the spectrum was not used to determine the presence of hydrogen bonding between carboxylic acid and cellulose since cellulose contains a large proportion of hydrogen bonds and could mask the existence of any new hydrogen bonds. The FTIR spectral results are in agreement with that of the NMR spectroscopic data, leading to the conclusion that ester bonds are, in fact, forming and hydrogen bonding may be occurring during melt-processing of MAPP and cellulose.

2.4.3 Lignin/MAPP blend

The lignin/MAPP blend was analyzed via the same methods as the cellulose/MAPP blend. The lignin sample used in this study was a commercial kraft lignin of softwood origin. Table 2.4 shows the results for ^{13}C NMR spectroscopic chemical shifts and $^{H}T_{1\rho}$ of lignin, MAPP and its blend. The same behavior seen for the cellulose/MAPP blend was observed in the lignin/MAPP blend (Figure 2.9). A new signal at 32.7ppm and the anhydride peak at 173.5ppm although much more pronounced and broader in the blend was observed than in the neat MAPP, while the peak at 180.1ppm was of lower intensity but broader. Again, the changes in the peaks at 180.1ppm and 173.5ppm may be from either a change in the ratio of species; diacid versus anhydride; a change in their relaxation times, esterification between MAPP and lignin, or hydrogen bonding.

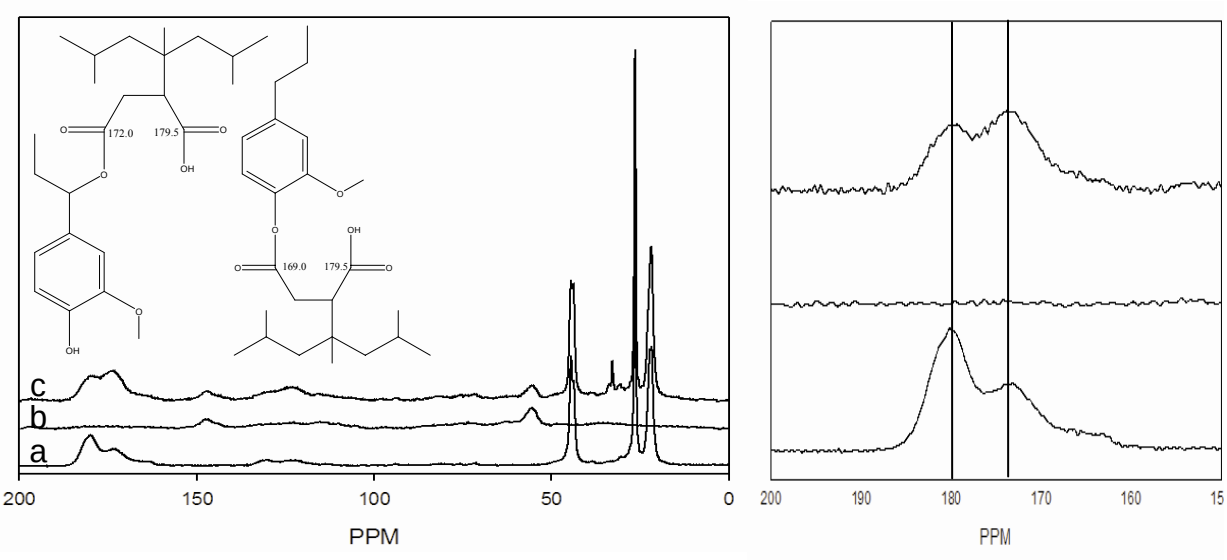

Figure 2.9 ^{13}C NMR spectra of (a) MAPP, (b) lignin and (c) MAPP/lignin blend and proposed structures of esterification between MAPP and lignin and close up of carbonyl region.

As with cellulose, the change in pH of the blend could cause a change in the equilibrium between the diacid, 180.1ppm and the anhydride, 173.5ppm. An increase in the anhydride form

would lead to a greater intensity of the peak at 173.5ppm and a decrease in the peak at 180.1ppm, as observed in the NMR spectrum of the blend. In order to determine if acidic conditions introduced by the lignin, pH = 6.0, affect the equilibrium, the pKa's of succinic acid was used (MeadWestvaco). Using the Equation 2.4 and the pKa of 4.16 to account for both carboxyl groups, as before, it was determined that the ratio of diacid to anhydride species in a pH of 6.0 was 69.2 (Vollhardt and Schore 1999). In order for more anhydride to form the pH would need to be below 4.16, otherwise the environment favors that of the diacid form. The spectrum of the lignin/MAPP blend shows no obvious increase in the signal at 180.1ppm associated with the diacid form of MAPP, thus the change in intensities was not due to a shift in the MAPP equilibrium.

Using ChemDraw Ultra to predict chemical shifts, it was determined that an esterification reaction between MAPP and lignin would lead to signals with chemical shifts at 169.0ppm, 172.0ppm and 179.5ppm. These shifts would overlap the already present MA signals of MAPP, leading to a change in intensity of these peaks. The conversion of the anhydride group of MAPP to an ester with the lignin, based on these chemical predictions would lead to the increase in the peak at 173.5ppm and conversely a decrease in the 180.1ppm peak. The behavior seen in the NMR spectrum is consistent with the chemical predictions, therefore leading to the possible conclusion that esterification between MAPP and lignin is also occurring.

As with cellulose the remaining carboxyl group left after esterification may be able to hydrogen bond with the lignin. Based on the complex structure of lignin there are several different possibilities for hydrogen bonding, although a change in chemical shift is unlikely to be seen as there is a large amount of intra-molecular H-bonding within lignin alone. A broadening

of the peaks at 173.5ppm and 180ppm is seen indicating that hydrogen bonding may be simultaneously occurring.

Table 2.4 ^{13}C NMR data for lignin/MAPP blend

Chemical Shifts for Lignin/MAPP blend (ppm)					Relaxation Time ($^{H}T_{1\rho}$, ms)			
Peaks (ppm)	**MAPP**	**Lignin**	**Lignin/ MAPP**	**ppm change**	**MAPP**	**Lignin**	**Lignin/ MAPP**	**$^{H}T_{1\rho}$ change**
180	180.1±0.3		179.6±0.4		3.6±0.3A		4.1±1.0AC	
173	173.5±0.1		173.9±0.4		3.9±0.1A		5.0±0.5BA	1.1ms
147		147.5±0.2	147.2±0.6			12.8±0.9A		
123		123.4±1.1	123.8±0.7			13.2±1.5A		
115		115.2±0.3	115.9±1.0			8.8±0.4B		
73		73.6±0.7				7.3±0.6B		
55		55.6±0.2	55.4±0.2			7.9±0.2B	6.4±0.2, A	1.5ms
44	44.4±0.3		44.3±0.2		5.3±0.3B		5.1±0.3BA	
32.7			32.7±0.2	New Peak			3.5±0.8, C	New Peak
26	26.4±0.3		26.3±0.3		5.4±0.3B		5.5±0.2BA	
21	21.9±0.3		21.8±0.3		4.9±0.1B		4.8±0.3BC	

A change in the relaxation time, $^{H}T_{1\rho}$, of both the peaks at 180.1ppm and 173.5ppm could cause the same change in peak intensities seen in the NMR spectrum of the lignin/MAPP blend. The $^{H}T_{1\rho}$ of the peak at 173.5ppm shows an increase of 1.1 ms (Table 2.4) indicating that the change in intensity was due to not only esterification, but in part to a change in relaxation time. The lack of change in the relaxation time of the peak at 180.1ppm in conjunction with the decrease in intensity of this peak, and the increase in the peak at 173.5ppm is further evidence of the possibility of esterification between MAPP and lignin. Possible evidence of hydrogen bonding can be seen with the change in the relaxation time of the methoxy group of the lignin at 55.4ppm. The $^{H}T_{1\rho}$ of this peak has a decrease of 1.5 ms indicating its molecular motion has changed. This methoxy group may hydrogen bond with the MAPP allowing for this change in relaxation time to occur. Not all of the characteristic lignin peaks in the blend were evaluated for $^{H}T_{1\rho}$ due to low peak intensity, the marked decrease in relaxation time of the methoxy peak at

55.4ppm allows for the possibility of homogeneity within the blend. Homogeneity (spin diffusion) or similar molecular motions are observed by the similarities of $^{H}T_{1\rho}$ data seen between all carbons of the MAPP and the lignin upon blending. Based on the NMR spectroscopic data above it can be concluded from the change in intensities of the MA peaks at 180.1ppm and 173.5ppm, the chemical shift predictions of esterification, the broadening of the peaks, as well as the heat and acidity of the environment that esterification and hydrogen bonding between MAPP and lignin was occurring.

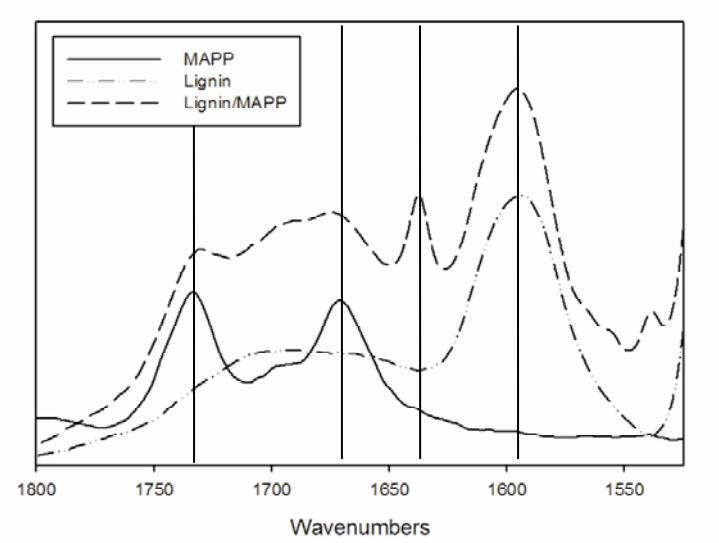

Figure 2.10 FTIR spectra of MAPP, lignin, and lignin/MAPP blend

Table 2.5 FTIR bands and ratios* for Lignin/MAPP blend

Band (cm^{-1})	Band Type	Lignin/MAPP Intensity/Area	MAPP Intensity/Area
1731	asymmetric anhydride stretch	1.00	1.00
1694	non H-bonded carboxylic acids	1.11(±0.02) / 1.00(±0.08)	0.52(±0.05) / 0.30(±0.04)
1673	symmetric anhydride stretch carboxylic acid stretch	1.16(±0.02) / 1.02(±0.12)	0.94(±0.01) / 0.98(±0.04)
1637	lignin/MAPP ester bonds	1.25(±0.15) / 0.76(±0.14)	

*ratios normalized to area and intensity of 1733cm^{-1}

The FTIR spectra of lignin/MAPP blend was compared with that of MAPP (Figure 2.10). While no bands have a significant shift in position, a new band was observed in the blend at 1637 cm^{-1} (Table 2.5). This band may be attributed to an ester bond. Kazayawoko (1999) saw a

presence of ester bonds with bleached kraft pulp (BKP) at 1722 cm^{-1}. For labeled ^{13}C MAPP this signal will correspond to a band at approximately 1650 cm^{-1}. This prediction is very close to that of the newly formed sharp band at 1637cm^{-1}, allowing for the determination that there is possible esterification occurring between lignin and MAPP. The ratios for area and intensity between 1694/1731were also examined and determined to be 1.11 and 1.00. These are higher than that of MAPP and alone and point to possible bonding. The ratios for area and intensity between 1671/1731 were 1.16 and 1.02 (Table 2.5). While these ratios indicate that there may be covalent bonding, the overlap of the lignin bands with that of the MAPP bands in the blend to not allow conclusive proof that esterification is occurring. The ratio between 1637/1731 was also examined as this is a new band and appears to indicate esterification. For intensity and area the ratios were 1.25 and 0.76 respectively. The larger ratios for 1671/1731 and 1694/1731 as well as the new band at 1637 appear to indicate that esterification between MAPP and lignin is occuring. However, the type of ester linkage (aliphatic or aromatic) could not de deduced from the spectra. The presence of hydrogen bonds cannot be detected due to the large overlap in the region of 1694cm^{-1}. Again, this data supports the previous conclusion that MAPP and lignin are esterified to some extent.

2.4.4 Maple/MAPP blend

Maple is a hardwood and contains both cellulose, lignin and many other hemicelluloses and extractives (Siöström, 1993). One of the hemicelluloses to consider is O-acetyl-4-O-methylglucurono-xylan which may contribute to acetate ester signals and carboxylic acid signals in the FTIR or NMR spectra. In the maple/MAPP blend, the same changes seen in both the cellulose and lignin blends are observed (Figure 2.11). The new peak at 32.6ppm is present (

Table 2.6) and much larger in the maple/MAPP blend than has been seen before, indicating a new, smaller methylene based carbon chain is present. The presence of the O-acetyl-4-O-methylglucurono-xylan hemicellulose is not seen in the carbonyl region in maple alone so the affect of these groups on the shape of the MA peaks can be ignored.

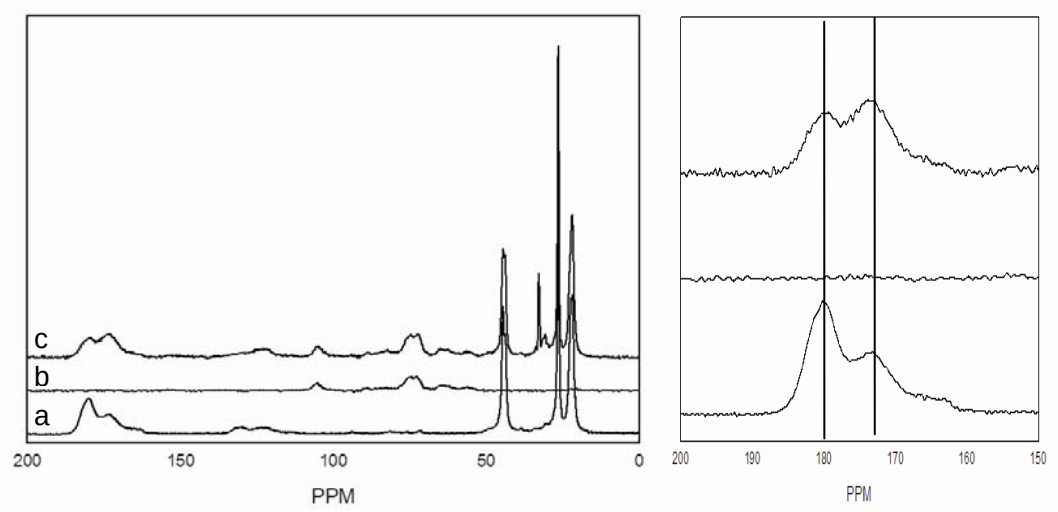

Figure 2.11 ^{13}C NMR spectra and close up of carbonyl region of (a) MAPP, (b) maple and (c) maple/MAPP blend.

As seen with both cellulose and lignin the peak at 173.5ppm again was of much larger intensity and broader than in the neat MAPP alone, while the peak at 180.1ppm decreased in intensity and is much broader. The reasons for the intensity changes, as seen before, may be due to a change in ratio of species, esterification, a change in relaxation time, or hydrogen bonding. The influence of the pH of maple was examined to rule out any changes in ratio of species due to the acidity of the environment. Maple has a pH of 5.3 which is lower than both cellulose and lignin, leading to a ratio of 13.8 between diacid and the anhydride form of MAPP, indicating there should be a larger concentration of the diacid instead of the anhydride, which the opposite is seen in the NMR spectrum (Gindl and Tschegg, 2002).

Table 2.6 13C NMR data for the maple/MAPP blend

Chemical Shifts for Maple/MAPP blend (ppm)					Relaxation Time ($^{H}T_{1\rho}$, ms)			
Peaks	**MAPP**	**Maple**	**Maple/ MAPP**	**ppm change**	**MAPP**	**Maple**	**Maple/ MAPP**	**$^{H}T_{1\rho}$ change**
180	180.1±0.3		179.8±0.2		3.6±0.3, A		3.1±0.3, A	
173	173.5±0.1		173.4±0.2		3.9±0.1, A		3.5±0.2, AB	0.4ms
105		105.4±0.1	105.1±0.4			7.1±0.3, A	4.3±0.3, BC	2.8ms
83		83.6±0.7	82.5±0.4			6.9±0.4, A		
73		73.3±1.2	74.7±0.4			6.9±0.3, A	4.1±0.5, BC	2.8ms
64		64.4±0.9	65.3±0.6			7.3±0.9, A		
55		55.6±0.6	56.4±0.3			11.1±1.2, B		
44	44.4±0.3		44.3±0.2		5.3±0.3, B		4.3±0.2, BC	1.0ms
32.6			32.6±0.2	New Peak			3.8±0.5, AB	New Peak
26	26.4±0.3		26.3±0.2		5.4±0.3, B		5.0±0.3, C	
21	21.9±0.3		21.8±0.3		4.9±0.1, B		4.3±0.3, BC	0.6ms
20		20.4±0.2						

Esterification and hydrogen bonding between the maple and the MAPP would cause similar chemical shifts as seen in the cellulose and lignin /MAPP blends, as these are two main components of maple. In fact, the spectrum of the maple/MAPP blend is a combination of the spectra of the cellulose/MAPP and lignin/MAPP blends. The broadening of the peaks at 180.1ppm and 173.5ppm and intensity changes of these peaks were consistent with predictions for esterification between cellulose and lignin, and the expected broadening of peaks due to hydrogen bonding. This finding leads to the conclusion that esterification and hydrogen bonding are likely occurring between maple and MAPP.

Now, upon blending the $^{H}T_{1\rho}$ of some cellulose carbons (C_1-105.1ppm; C2, C3, C5-74.7ppm) along with the $^{H}T_{1\rho}$ of the peak at 173.5ppm have significant decreases in relaxation time; upon blending the motional characteristics of these carbons are therefore changing. In addition most carbons have the similar $^{H}T_{1\rho}$; denoted by A,B,C; which was seen in both the cellulose and lignin blends, indication similar motional characteristics are allowing for intimate molecular meshing between the maple and the MAPP, supporting the idea of molecular interactions between the two as a result of esterification and/or hydrogen bonding. The

similarities in the behavior of the cellulose and lignin MAPP blends with the maple/MAPP blend as well as chemical predictions and the compatibility of relaxation times all points to esterification and hydrogen bonding between maple and MAPP.

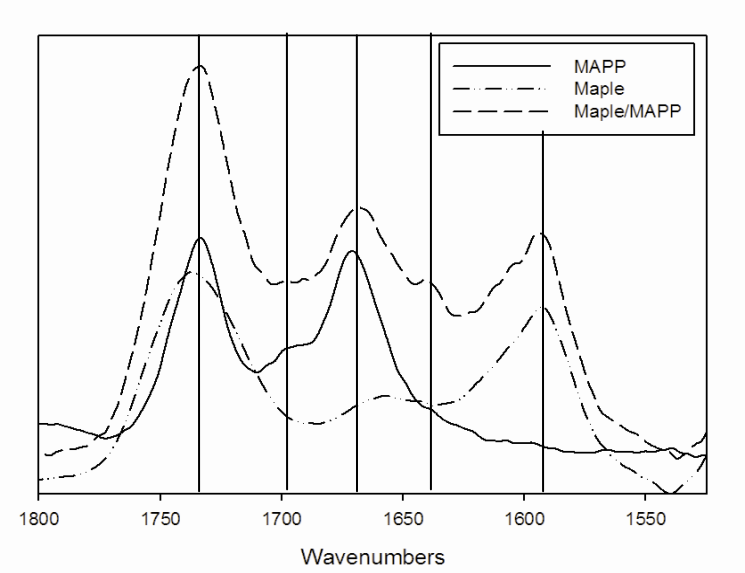

Figure 2.12 FTIR spectra of MAPP, maple, and maple/MAPP blend

Table 2.7 FTIR bands and ratios* for Maple/MAPP blend

Band (cm^{-1})	Band Type	Maple/MAPP Intensity/Area	MAPP Intensity/Area
1734	asymmetric anhydride stretch	1.00	1.00
1698	non H-bonded carboxylic acids	0.51(±0.02) / 0.22(±0.03)	0.52(±0.05) / 0.30(±0.04)
1669	symmetric anhydride stretch carboxylic acid stretch	0.66(±0.01) / 0.52(±0.03)	0.94(±0.01) / 0.98(±0.04)
1639	lignin/MAPP ester bonds	0.94(±0.08) / 0.76(±0.05)	

*ratios normalized to area and intensity of $1733cm^{-1}$

The FTIR spectral data for the maple/MAPP blend again shows a new and very sharp band at $1639cm^{-1}$ (Figure 2.12) while the anhydride bands are overlapped by bands in the maple (Table 2.7). This is an indication of esterification between the labeled MAPP and maple. This is consistent with the new band seen in the lignin/MAPP blend allowing for both the ability for lignin and cellulose/hemicellulose to bond with MAPP. A point to note is that the hemicellulose,

O-acetyl-4-O-methylglucuronoxylan, present in approximately 25-30% in maple could also react with MAPP to form ester linkages (Siöström, 1993). An ester band due to bonding with cellulose and/or hemicellulose and a band for hydrogen bonding overlap with bands present in maple. Although there is a large amount of overlap with MAPP and maple the ratios for intensity and area between 1669/1734 were calculated at 0.66 and 0.52, while the ratios for 1700/1734 were 0.51 and 0.22 (Table 2.7). These ratios are lower than what was seen in MAPP alone. This is not surprising due to the large overlap directly on top of the MAPP bands. Due to this large overlap no conclusion can be easily drawn from the ratios. Although the new band at 1639cm^{-1} points directly to esterification between MAPP and maple, and the ratios of intensity are area for 1639/1734 were 0.94 and 0.76. These results are very consistent with the results obtained from the NMR spectroscopic data, including the similarities between the cellulose and lignin blends with that of the maple/MAPP blend. In the end, it can be concluded that MAPP does in fact participate in esterification and most likely hydrogen bonding with maple, and therefore it is probable that MAPP will do the same with other wood species.

2.5 Conclusions

The cellulose/MAPP, lignin/MAPP, and maple/MAPP blends all show distinct evidence of esterification and hydrogen bonding. In previous research esterification has been seen only between cellulose, TMP fibers, and BKP fibers with MAPP, while the presence of esterification between lignin and wood with MAPP during melt processing was not seen previously. This study shows that the use of NMR spectroscopy and FTIR spectroscopy as analytical tools for detecting esterification and hydrogen bonding on a melt-mixed WPC is not only possible but

provides information about these composites that was not previously detectable via other methods.

Acknowledgements

This work was sponsored by the Office of Naval Research, under the direction of Mr. Ignacio Perez, under Grant N00014-03-1-0949.

The WSU NMR Center equipment was supported by NIH grants RR0631401 and RR12948, NSF grants CHE-9115282 and DBI-9604689 and the Murdock Charitable Trust.

2.6 References

Avella M, Casale L, Dell'erba R, Focher B, Martuscelli E, Marzetti A. 1998. Broom fibers as reinforcing materials for polypropylene-based composites. Journal of Applied Polymer Science. 68: 1077-1089

Bratawinjaja AS, Gitopadmoyo I. 1989. Adheson property of polypropylene modified with maleic anhydride by extrution molding. Journal of Applied Polymer Science, 37: 1141-1145

Carlborn K, Matuana LM. 2006. Functionalization of wood particles through a reactive extrusion process. Journal of Applied Polymer Science, 101: 3131-3142.

Deligio, T. 2006. Wood-plastic composites build new markets. Modern Plastics,

Felix, JM, Gatenholm P. 1991. The nature of adhesion in composites of modified cellulose fibers and polypropylene. Journal of Applied Polymer Science, 42: 609-620

Gil, AM, Neto CP. 1999. Solid-state NMR studies of wood and other lignocellulosic materials. Annual Reports on NMR Spectroscopy.

Gindl M, Tschegg S. 2002. Significance of the acidity of wood to the surface free energy components of different wood species. Langmuir, 18: 3209-3212.

Harper DP, Wolcott MP. 2006. Chemical imagining of wood-polypropylene composites. Applied Spectroscopy, 60: 898-905.

Heinen W, Erkens SW, van Duin M, Lugtenburg J. 1999. Model compounds and ^{13}C NMR increments for the characterization of maleic anhydride-grafted polyolefins. Journal of Polymer Science: Part A: Polymer Chemistry. 37: 4368-4385

Heinen W, Rosenmöller CH, Wenzel CB, de Groot JM, Lugtenburg J, van Duin M. 1996. ^{13}C NMR study of the grafting of maleic anhydride onto polyethylene, polypropylene, and ethane-propene copolymers. macromolecules. 29: 1151-1157

Joly C, Gauthier R, Escoubes M. 1996. Partial masking of cellulosic fiber hydrophilicity for composites. Water sorption by chemical modified fibers. Journal of Applied Polymer Science, 61: 57-69

Kazayawoko M, Balatinecz JJ, Woodhams RT. 1997. Diffuse reflectance Fourier transform infrared spectra of wood fibers treated with maleated polypropylenes. Journal of Applied Polymer Science, 66: 1163-1173.

Kazayawoko M., Balatinecz JJ, Matuana LM. 1999. Surface modification and adhesion mechanisms in woodfiber-polypropylene composites. Journal of Materials Science, 34: 6189-6199.

Macomber RS. 1998. A complete introduction to modern NMR spectroscopy. New York: Wiley Interscience John Wiley & Sons, Inc.

Maunu SL. 2002. NMR studies of wood and wood products. Progress in Nuclear Magnetic Resonance Spectroscopy, 40: 151-174.

Matías MC, De La Orden MU, Sánchez CG, Urreaga JM. 2000. Comparative spectroscopic study of the modification of cellulosic materials with different coupling agents. Journal of Applied Polymer Science, 75: 256-266.

Parker AA, Marcinko JJ, Sheih YT, Shields C, Hedrik DP, Ritchey WM. 1989. Studies of polymer morphology with ^{13}C inversion recovery cross polarization NMR. Polymer Bulletin, 21: 229-234.

Pavia DL, Lampman GM, Kriz GS. 1996. Introduction to spectroscopy: A guide for students of organic chemistry. Orlando: Harcourt Brace College Publishers.

Poptoshev E, Rutland MW, Claesson PM. 2000. Surface forces in aqueous polyvinylamine solutions. 2. Interactions between glass and cellulose. Langmuir, 16, 1987

Qui W, Endo T, Hirotsu T. 2006. Interafcial interaction, morphology, and tensile properties of a composite of highly crystalline cellulose and maleated polypropylene. Journal of Applied Polymer Science, 102: 3830-3841.

Qui W, Endo T, Hirotsu T. 2004. Interafcial interactions of a novel mechanochemical composite of cellulose and maleated polypropylene. Journal of Applied Polymer Science, 94: 1326-1335.

Qui W, Zhang F, Endo T, Hirotsu T. 2004. Milling-induced esterification between cellulose and maleated polypropylene. Journal of Applied Polymer Science, 91: 1703-1709.

Qui W, Zhang F, Endo T, Hirotsu T. 2005. Effect of maleated polypropylene on the performance of polypropylene/cellulose composites. Polymer Composites, 26: 448-453.

Sanadi AM, Rowell RM, Young RA. 1992. Estimation of fiber-matrix interfacial shear strength in lignocellulosic-thermoplastic composites. Materials interactions relevant to recycling of wood-based materials (Vol. 266), Eds. Rowell, R. M.; Laufenberg, T. L. and Rowell, J. K. pp81-92

Schmidt-Rohr K, Spiess HW. 1994. Solid state NMR and polymers. San Diego: Academic Press.

da Silva MM, Tavares MIB, Stejskal EO. 2000. ^{13}C-detected ^{1}H spin diffusion and ^{1}H relaxation study of multicomponent polymer blends. Macromolecules, 33: 115-119.

Sjöström E. 1993. Wood chemistry fundamentals and applications second edition. San Diego: Academic Press.

Takase S, Shiraishi N. 1989. Studies on composites from wood and polypropylenes. II. Journal of Applied Polymer Science. 37: 645-659

Vollhardt, K. Peter C., Neil E. Schore. 1999. Organic Chemistry: Structure and Function, Third Edition. New York : W. H. Freeman and Company.

Wolcott M, Chowdhury M, Harper D, Li T, Heath R, Rials T. 2000. Coupling agent/lubricant interactions in commercial wood plastic formulations. The Sixth International Conference on Woodfiber-Plastic Composites, 197-204.

Wu HD, Ma CCM, Chang FC. 2000. The solid state 13C NMR studies of intermolecular hydrogen bonding formation in a blend of phenolic resin and poly(hydroxyl ether) of bisphenol A. Macrololecular Chemical Physics. 201: 1121.

Chapter 3 Evaluation of Interaction between MAPP, Lubricants, and MAPP Zinc Stearate Wood Polymer blends

Abstract

Maleic anhydride polypropylene (MAPP) is a commonly used coupling agent in polypropylene based WPCs, while ethylene bisstearamide (EBS), the ester based Optipak 100 (OP100) and zinc stearate (ZnSt) are widely used lubricants. It has been noted in practice that the use of MAPP significantly increases the mechanical properties in PP based WPCs. However, that is with MAPP alone; the use of the lubricant ZnSt with MAPP drastically decreases the improvement that is seen in the mechanical properties. As for EBS and OP100, no change in mechanical properties is seen. The chemical interactions between MAPP and wood polymers were previously studied with solid state nuclear magnetic resonance spectroscopy and Fourier transform infrared spectroscopy, and it was determined that esterification and hydrogen bonding occur between MAPP and wood polymers (Chapter 2). Currently there is only a limited amount of information on the repercussions of using lubricants in conjunction with the coupling agent, MAPP. This study examined the interactions between MAPP and lubricants. EBS and OP100 were each blended with MAPP and no covalent bonding was found to have occurred between the EBS and MAPP or between OP100 and MAPP. There was however, hydrogen bonding between the amide functionalities of EBS and the MA moieties of MAPP as well as between the ester groups of OP100 and the MA moieties of. The ZnSt was found to form anhydride bonds with MAPP. Based on this the study of ternary blends was warranted to determine if MAPP/wood interactions may be hindered by this ZnSt/MAPP interaction. It was determined that in all three blends (ZnSt/MAPP/Cellulose, ZnSt/MAPP/Lignin, ZnSt/MAPP/Maple) the ZnSt/MAPP interaction far overpowered the wood/MAPP interactions. The formation of stearic acid was found in the ZnSt/MAPP/Maple blend, and that the formation of stearic acid is catalyzed by the

presence of MAPP. The favored reaction between the MAPP and the ZnSt decreases the efficacy for MAPP to bond with wood and therefore explains the reasons behind the decrease in mechanical properties seen in WPCs containing MAPP and ZnSt.

Introduction

Considerable research has been performed to improve interfacial adhesion including the addition of a coupling agent into the composite. Maleic anhydride polypropylene (MAPP) is a widely used coupling agent within polypropylene based composites. The addition of MAPP shows a marked increase in the modulus of rigidity, MOR, and modulus of elasticity, MOE, of polypropylene, PP, based composites due to esterification and hydrogen bonding between the MAPP and the wood or wood polymers (Chapter 2).

Wood plastic composites contain not only wood and plastic but frequently a coupling agent and a lubricant as well. Lubricants are used in order to enhance the ability of the components to pass into and then through the extruders unhindered as well as lead to a smoother and more desirable surface. The three major lubricants used are EBS, OP100 and zinc stearate (ZnSt). Interestingly, when EBS and OP100 lubricants are used in conjunction with MAPP, the performance enhancement usually imparted by MAPP is preserved (Wolcott, 2000). On the other hand, when ZnSt lubricant is used in conjunction with MAPP, the MAPP performance enhancement is completely annihilated. This suggests that ZnSt interferes with the coupling mechanism of MAPP (Wolcott, 2000). To date, only two studies have been conducted to try and understand the mechanisms of interference of lubricants on MAPP adhesion enhancement mechanism.

Harper et al determined that wood (in this case maple) provides a surface on which the polypropylene (PP) can nucleate. After nucleation these crystals impinge on one another as they

grow creating a transcrystalline later (TCL). Adding MAPP as a coupling agent to a PP/wood blend increases the nucleating ability of the wood fibers over that of the neat PP. The MAPP collects at the edge of the TCL and increases adsorption of the surface thereby increasing the mechanical properties of the composite. The addition of a mix of ZnSt/EBS to a wood/PP/MAPP blend showed a a significant decrease in the nucleating ability of the wood. On the other hand, the addition of OP100 to the wood/PP/MAPP blend leads to a greater nucleating ability over that of the ZnSt/EBS blends (Harper, 2004). Harper et al determined there is little interaction between the MAPP and EBS or OP100, while FTIR spectroscopic data showed that ZnSt may hydrolyze MAPP, creating the much less reactive dicarboxylic acid seen at 1712 cm^{-1}. Also the formation of hydrogen bonds between wood and MA may not be as favored as the hydrogen bonds between MA and other hydrolyzed copolymers, such as ZnSt. This is suspected to be the cause of the poor interaction and mechanical properties seen in composites when ZnSt is used. The possibility of co-crystallization between the MAPP and the PP is also thought to be a cause for the increased mechanical properties seen when MAPP is used as a coupling agent in PP based WPCs (Harper, 2006). A second spectroscopic method would be useful to identify any interactions.

Solid State ^{13}C NMR spectroscopy was used in our previous study (Chapter 2) and has been particularly useful for the study of solid phase polymers as it gives detailed information of the types of functional groups present through the chemical shifts seen in the resulting spectrum, as well as morphological information (Parker et al, 1989). If a change in chemistry occurs a change in chemical shift may be seen. Another sign of a change in chemistry is a change in the peak shape or intensity. Furthermore, intimacy between polymer phases or nanoscale morphology in polymer blends can be determined via relaxation time measurements, such as

proton spin lattice relaxation in the rotating frame $^{H}T_{1\rho}$s (Silva et al, 2000). Upon blending two polymers, a change in $^{H}T_{1\rho}$ in the individual polymers, may indicate a change in the molecular motion of the polymer possibly due to molecular interactions. Similar $^{H}T_{1\rho}$s of different carbons in a polymer blend measured through carbons pertaining to each of the polymer, indicates either a similar motional regime or homogeneity on a nanoscale level induced by spin diffusion. Therefore, $^{H}T_{1\rho}$ measurements are another way to probe intimacy and interactions between MAPP and wood polymers by solid state NMR spectroscopy.

To determine $^{H}T_{1\rho}$ associated with each carbon a variable contact time cross-polarization pulse can be used. The intensity of each peak is plotted against the contact time and the magnetization equation below is then used to fit the resulting curve allowing for the $^{H}T_{1\rho}$ for each peak to be obtained (Schmidt-Rohr and Spiess, 1994).

Equation 3.1 Magnetization Equation

$$I(t) = I * (^{H}T_{1\rho} / (^{H}T_{1\rho} - T_{CH}))(\exp^{-t/T_{1\rho}} - \exp^{-t/T_{CH}})$$

The $^{H}T_{1\rho}$s determined for each peak can then be compared with that of the same peaks in a blend or after a reaction to determine if motional characteristics have changed.

The chemical interactions between MAPP, wood, wood polymers were studied via ^{13}C CPMAS NMR spectroscopy and FTIR spectroscopy (Chapter 2). As this study was successful in the determination of chemical interactions between wood and MAPP, the interaction between MAPP and the three major lubricants may be determined by solid state NMR spectroscopy as well. The interactions occurring between ternary blends of MAPP, wood polymers, and lubricants was also studied in an effort to determine which interaction would dominate; MAPP-ZnSt or MAPP-wood. The determination of the interactions between MAPP, lubricants and wood can aid in designing better coupling agents and in the determination of which lubricant system to use based on the coupling agents for WPCs.

3.3 Experimental

3.3.1 Materials

Solid State ^{13}C CP NMR spectroscopy only detects the ^{13}C form of carbon which is of 1% natural abundance. With even a small amount of MA grafted onto the PP backbone the detection of the MA would be very low. To increase the visibility of the MA functional group 100% ^{13}C enriched MAPP at the C1 and C4 carbons. The ^{13}C labeled MAPP was provided by Honeywell and patterned after the A-C® 950, a commercial product. The SAP (saponification number) of the final product was approximately 41.2 mg KOH/gm (3.6 wt % MA) with a viscosity of 2,200 cps at 190 °C. The C1 and C4 carbons were chosen because they are the functional groups that are believed to be involved in the coupling mechanisms. The OP100, EBS, ZnSt, cellulose (powder, Fisher)), pine kraft lignin (Indulin AT), maple (American Wood Fibers), and stearic acid (Fisher) were all purchased commercially.

3.3.2 Sample Preparation

As done in the previous study (Chapter 2) the ^{13}C labeled MAPP, OP100, EBS, and ZnSt were dried under vacuum to a constant weight and stored under vacuum, as were the resulting heated components and the blends. To determine MAPP/lubricant interaction three blends were made at a weight ratio of 1:1, OP100/MAPP, EBS/MAPP, and ZnSt/MAPP. The tertiary blend made were also at a 1:1:1 ratio and consisted of ZnSt/MAPP/cellulose, ZnSt/MAPP/lignin, or ZnSt/MAPP/maple. Before the blends were processed unlabeled blends were used to remove any impurities from the injection molder. The ^{13}C labeled blends were mixed via a Dynisco Laboratory Mixing Molder (injection-molder). The samples were processed at 180°C and 50

rpm for 2 minutes, minimizing thermal degradation of the components. These samples were then divided into three separate replicates that were deemed for CP/MAS and FTIR spectroscopic analysis. Furthermore, control samples consistent of the neat components, MAPP, EBS, OP100, ZnSt, and stearic acid, as well as cellulose, lignin, and maple that had been heated in an oven at 180˚C for 2 minutes, were evaluated for comparison with the blends; these components will be considered neat components.

3.3.3 NMR Spectroscopy

All NMR spectroscopy experiments were performed on a Bruker Avance 400 with a Chemagnetics 7.5mm double resonance probe under the same parameters as the previous study (Chapter 2). Once changes were determined all neat components as well as the blends were subjected to variable contact time experiments. CP experiments with variable contact times were performed and the data was then plotted and curve fit using OriginPro7 according to Eq. 1 in order to determine $^{H}T_{1\rho}$ of each identifiable carbon, T-tests were used to determine significant changes ($p \leq 0.05$) in $^{H}T_{1\rho}$ within a system and also before and after blending. Tukey tests were also used to determine similarity between relaxation times to group the peaks, indicated by the letters A, B, C... after the reported relaxation time.

3.3.4 FTIR Spectroscopy

FTIR spectroscopy has been used by Harper et al and in our previous study (Chapter 2) as described above to determine the presence of ester bonds between MAPP and cellulose as well as the determination of possible interaction between MAPP and ZnSt, it was again used in this

study to aid in determination of new bonds between MAPP and the lubricants. The FTIR spectra were collected using a ThermoNicolet Avatar 370 spectrometer (Thermo Electron Corporation), in the attenuated total reflection (ATR) mode (SmartPerformer, ZnSe crystal). The absorbance spectra were mathematically ATR corrected using the Omnic 7.0 software package. Each spectrum was taken as an average of 64 scans at a resolution of 4 cm^{-1}, with three replicates of each sample.

3.4 Binary blends: Results and Discussion

3.4.1 MAPP Characterization

The structure of MAPP was studied extensively in Chapter 2. In summary it was determined that the peaks in the ^{13}C NMR spectrum at 173.5ppm and 180.1ppm belonged to the anhydride and diacid moieties, respectively, and outside the carbonyl region, the main chain carbons are observed at 44.4, 26.4 and 21.9ppm. The peak at 21.9ppm corresponds to the methyl group on PP, while the peak at 26.4ppm is the tertiary carbon and the final peak at 44.4ppm is the secondary carbon, joining tertiary carbons, (Figure 3.1). There are also two peaks that appear at 130ppm and 123ppm, identified by a * in the spectrum. These peaks are artifacts on the spectrum and are called spinning side bands, which are spaced at the spinning frequency from the isotropic shifts (180.1ppm, 173.5ppm), approximately mirror the shape of the isotropic shifts, and have a lower intensity (Macomber, 1998). Once the chemistry of MAPP was understood, its phase morphology could be evaluated by $^{H}T_{1\rho}$.

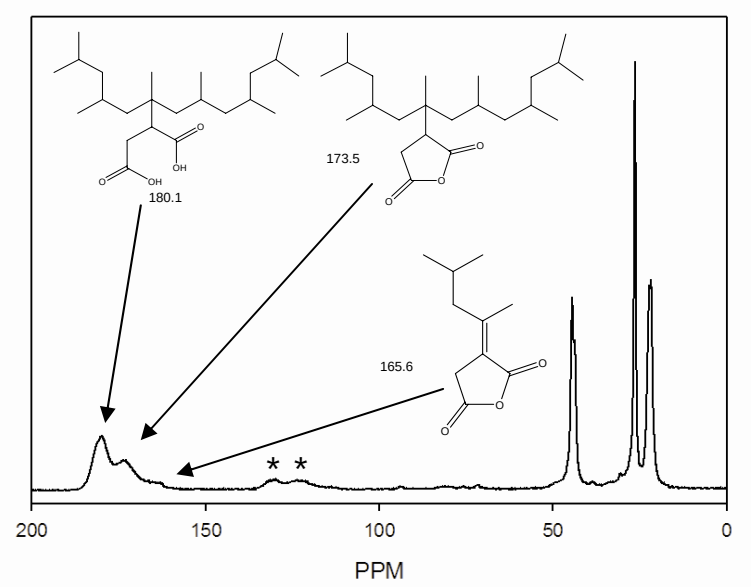

Figure 3.1 NMR spectra of ^{13}C MAPP

Table 3.2 contains the chemical shifts for neat ^{13}C MAPP as well as the $^{H}T_{1\rho}$ associated with each carbon. The relaxation times were grouped via the Tukey test to determine the level of homogeneity, and the groups are denoted A,B,C, etc. The two peaks corresponding to the functional groups of maleic anhydride have similar $^{H}T_{1\rho}$s, while the PP carbon peaks all have similar relaxation times, yet very different from the MA functional groups. From this it was concluded that the MA carbon groups have distinct molecular motion and are phase separated from the main chain PP. This type of behavior appears to reflect a structure in which the main chain PP entangles and crystallizes, excluding the MA groups from the PP structure.

Next FTIR spectra of the neat ^{13}C labeled MAPP was compared with that of ^{12}C MAPP. Based on the equation for reduced mass, the equation for the vibration frequency of a molecule, and the ratio of this frequency for the unlabeled and ^{13}C labeled MAPP, it was determined that the anhydride bands should be present at approximately 1740cm^{-1} and 1690cm^{-1} (Table 3.1),

while the normal ^{12}C bands would be seen at approximately 1810cm^{-1} and 1760cm^{-1}. compares the frequencies for ^{12}C, ^{13}C, and ^{12}C-^{13}C bonds for several carbonyl compounds.

Equation 3.2 Reduced mass

$$\mu = \frac{m_1 m_2}{m_1 + m_2}$$

Equation 3.3 Vibration frequency

$$\nu = \frac{1}{2\pi}\sqrt{\frac{k}{\mu}}$$

Table 3.1 Comparison of ^{12}C and ^{13}C vibrational frequencies

Functional Group	^{12}C* (cm^{-1})	^{13}C (cm^{-1})	^{12}C-^{13}C (cm^{-1})
Anhydride	1810, 1760	1740, 1690	1775, 1725
Ester	1735	1670	1700
Aldehyde	1725	1660	1690
Ketone	1715	1650	1680
Carboxylic acid: free/H-bonded	1760/1710	1690/1645	1725/1675
Acetate	1750	1680	1715
Amide	1690	1625	1655

*Pavia et al, 1996

From the FTIR spectrum below (Figure 3.2), the 2 anhydride bands of the labeled ^{13}C MAPP used in this study are present at 1733cm^{-1} and 1670cm^{-1}. The band at 1733cm^{-1} is the asymmetrical stretching band while the band at 1670cm^{-1} is the symmetrical stretching band. The hydrogen bonded carboxylic band appears at 1670cm^{-1} as well, indication that the band seen in the spectrum is a combination of both the anhydride and carboxylic bands. The shoulder seen at 1700cm^{-1} may be attributed to a small amount of non-hydrogen-bonded carboxylic acids. These non-hydrogen-bonded carboxylic acids would usually appear around 1760cm^{-1} in a ^{12}C compound, whereas in a ^{13}C compound they would appear around 1700cm^{-1} as seen in the spectrum. The ratios of area and intensity between 1733/1671 were calculated at 1.48 and 1.05, to aid in determination of new bonds. Also the ratios between 1733/1701 (1701 is the shoulder on 1670cm^{-1}) were found to be 2.05 and 1.73, respectively. The band seen at 1800cm^{-1} is not

included in the interpretation as it has a very low intensity and in standard practice bands with such low intensity are not included in interpretations.

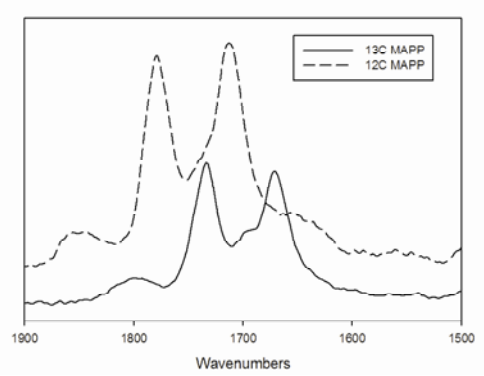

Figure 3.2 FTIR spectra of ^{12}C and ^{13}C MAPP

3.4.2 EBS/MAPP blend

The EBS/MAPP was first evaluated by ^{13}C NMR spectroscopy and the spectrum was first evaluated for any obvious changes in peak shape or intensity and then for the presence of a change in chemical shift. The chemical structure of EBS can be seen in Figure 3.3.

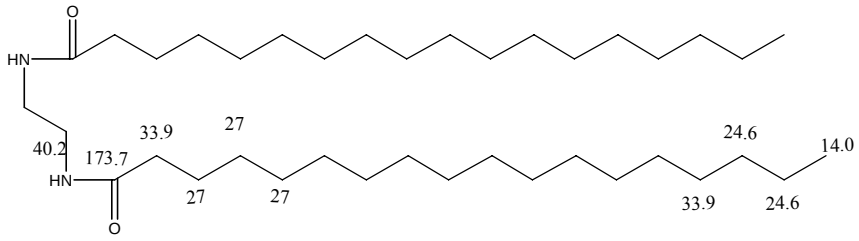

Figure 3.3 Chemical structure of EBS with predicted ^{13}C NMR spectroscopic chemical shifts

The spectrum of the EBS/MAPP blend when compared to that of the neat components shows an overlap of the EBS C=O peak with the MAPP anhydride peak at 173.5 ppm (Figure 3.4). Upon initial inspection it is noted that the overlapping chemical shifts at 173.5ppm lead to an increase in the intensity of that peak. This change in peak intensity appears to be due to a mere overlap of the C=O of the EBS and the anhydride of the MAPP, rather than a chemical interaction. The only statistically significant change in chemical shift was the main chain EBS peak seen at 33.9

shifting to 34.0 after blending, Table 3.2. This peak corresponds to the carbons directly next to the C=O carbons, and is likely due to a change in conformation of the structure. Based on the lack of change in the chemical shifts of the MA functional group it is unlikely that any chemical interactions are present between these two molecules.

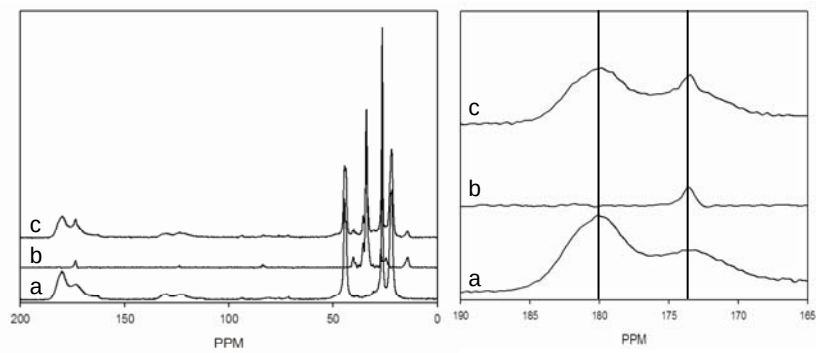

Figure 3.4 ^{13}C NMR spectra of a) MAPP; b) EBS; c) EBS/MAPP blend and an expanded view of the carbonyl region

Table 3.2 ^{13}C NMR data for EBS/MAPP blend

Chemical Shifts for EBS/MAPP blend (ppm)					**Relaxation Time ($^{H}T_{1\rho}$, ms)**			
Peaks ppm	**MAPP**	**EBS**	**EBS/MAPP**	**ppm change**	**MAPP**	**EBS**	**EBS/MAPP**	**$^{H}T_{1\rho}$ change**
180	180.1±0.3		180.0±0.5		3.6±0.3 A		3.7±0.4 A	
173	173.5±0.1	173.6±0.0	173.7±0.1		3.9±0.1 A	4.7±0.2 A	3.8±0.3 A	
44	44.4±0.3		44.4±0.0		5.3±0.3 B		5.1±0.2 B	
40		40.2±0.0	40.2±0.1			4.8±0.1 A	4.0±0.4 AC	0.8ms
33		33.9±0.0	34.0±0.0	0.1ppm		5.4±0.0 B	5.1±0.5 B	
27		27.0±0.0				4.9±0.2 A		
26	26.4±0.3		26.4±0.0		5.4±0.3 B		5.5±0.3 B	
24		24.6±0.0				5.4±0.1 A		
21	21.9±0.3		21.9±0.0		4.9±0.1 B		5.0±0.2 B	
14		14.3±0.0	14.3±0.1			6.5±0.3 C	5.0±0.3 BC	1.5ms

In order to further examine the blend for any changes in morphology the relaxation times were studied. The first thing to be noted in regards to the relaxation time is that the center two CH_2 groups of EBS, 40.2ppm, show a 0.8ms decrease in $^{H}T_{1\rho}$, and the terminal methyl of the EBS shows a 1.5 ms decrease as well. The decrease of the $^{H}T_{1\rho}$ for the carbons next to the amide group (40.2ppm) may indicate that there is H-bonding occurring between the MAPP and the

amide group of the EBS. This hypothesis is further supported by the fact that after blending $^{H}T_{1\rho}$ of the amide group is now statistically the same as those of the MA moieties of the MAPP. The MAPP shows no significant changes in $^{H}T_{1\rho}$ for any of the peaks and the phase separation present in the neat MAPP is seen in the blend (denoted A,B…), where the maleic moieties have a separate relaxation time from the PP chain. The EBS motional characteristics, on the other hand, are altered to some degree when crystallized in the presence of MAPP, as indicated by the decrease in $^{H}T_{1\rho}$ of the terminal methyl of the EBS (14.3ppm) and the amide groups (40.2ppm). Furthermore, there is a clear difference in the $^{H}T_{1\rho}$ of the carbonyl functional groups and the aliphatic groups, whether from MAPP or EBS. Namely, the carboxyl carbons have different motional characteristics than the aliphatic carbons showing segregation of polar and non polar carbons as previously observed in neat MAPP. To conclude, the NMR spectroscopic data shows that apart from a slight change in EBS conformation induced by the MAPP, no chemical interaction between EBS and MAPP exist, as was expected.

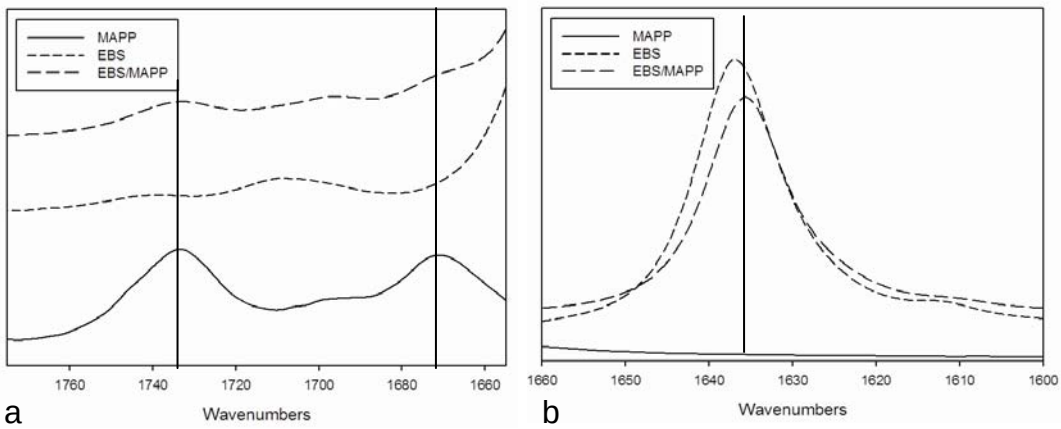

Figure 3.5 FTIR spectra expanded view of a) anhydride/carboxylic region of MAPP, EBS and EBS/MAPP blend and b) amide region of MAPP, EBS and EBS/MAPP blend

Table 3.3 FTIR bands and ratios* for EBS/MAPP blend

Band (cm^{-1})	Band Type	EBS/MAPP Intensity/Area	MAPP Intensity/Area
1733	asymmetric anhydride stretch	1.00	1.00
1695	non H-bonded carboxylic acids	1.14(±0.01) / 1.10(±0.06)	0.52(±0.05) / 0.30(±0.04)
1669	symmetric anhydride stretch carboxylic acid stretch	1.69(±0.02) / 1.44(±0.03)	0.94(±0.01) / 0.98(±0.04)

*ratios normalized to area and intensity of $1733cm^{-1}$

Next the FTIR spectra of the EBS/MAPP blend was reviewed. The anhydride and carboxyl bands of the MAPP almost disappear when blended with the EBS (Figure 3.5). This is due to the much greater intensity of the EBS amide band at $1637cm^{-1}$ (Table 3.3), it appears to have a $1cm^{-1}$ shift when blended, but this is much lower than the $4cm^{-1}$ resolution and therefore is not significant. EBS also shows a very low absorbing band at $1708cm^{-1}$, which is under the tail of the amide band that also overlaps the anhydride bands of MAPP. The absorbance of this band is so strong that even though it is not directly on top of the anhydride and carboxyl bands of the MAPP, the long tail of the amide band is still able to significantly overshadow them. Table 3.3 contains the ratios between the bands. The change in ratios seen appear to be due to the overlap of the tail of the EBS amide band and not due to a change in chemistry and therefore can not be conclusive. No clear indication of any covalent bonding between MAPP and EBS can be found, while evidence of H-bonding can be seen between the MA moieties and the amide groups of EBS. This indicates that there is some chemical interaction between MAPP and EBS, although it is unlikely that hydrogen bonding would affect the efficacy of MAPP. In fact, EBS has not been shown to reduce any mechanical properties of WPCs containing MAPP.

3.4.3 OP100/MAPP blend

Figure 3.6 shows the NMR spectra of OP100/MAPP blend compared to the neat components. As seen with the EBS/MAPP blend the C=O of the ester in OP100 overlaps with

the anhydride of the MAPP at 173.5ppm. Initially changes in the peak intensities were examined. It appears that there may be some shift from the diacid to the anhydride form of MAPP as the diacid peak appears to be somewhat diminished in intensity. The anhydride peak at 173.5ppm shows a marked increase, but there is significant overlap between the MAPP anhydride peak and the OP100 ester peak. While the true structure and therefore pKa of OP100 is not known the typical pKa for an ester is approximately 25, and far less reactive than an anhydride or carboxylic acid, usually requiring the presence of a catalyst to react (Vollhardt and Schore, 1999). Therefore the decrease in the diacid peak at 180ppm may be due to the shift towards more of the anhydride form of MAPP. As stated in previous work (Chapter 2) MAPP shifts towards the more reactive form when heated. It appears that not only is the change in peak intensity due to the overlap of the ester peak of OP100 and the anhydride peak of MAPP, but that the OP100 may be conducive to the ability of MAPP to form greater amounts of the anhydride form of MAPP under a heated environment.

Changes in chemical shift were also studied in order to determine if any new bonds had formed. No changes in chemistry of the functional groups are seen, as there is no shift of the peaks. In fact, little interaction can be seen in the OP100/MAPP blend, Table 3.4. The only change in chemical shift was the peak at 33.3ppm, main chain carbon peak of OP100 and likely from carbons directly next to the ester groups, shifted to 33.2ppm. Similar results were seen in the EBS/MAPP blend, where there were no changes in chemical shift other than a small change in the carbons directly next to the functional groups. This indicates that there may be a small change in the conformation of the main chain for OP100.

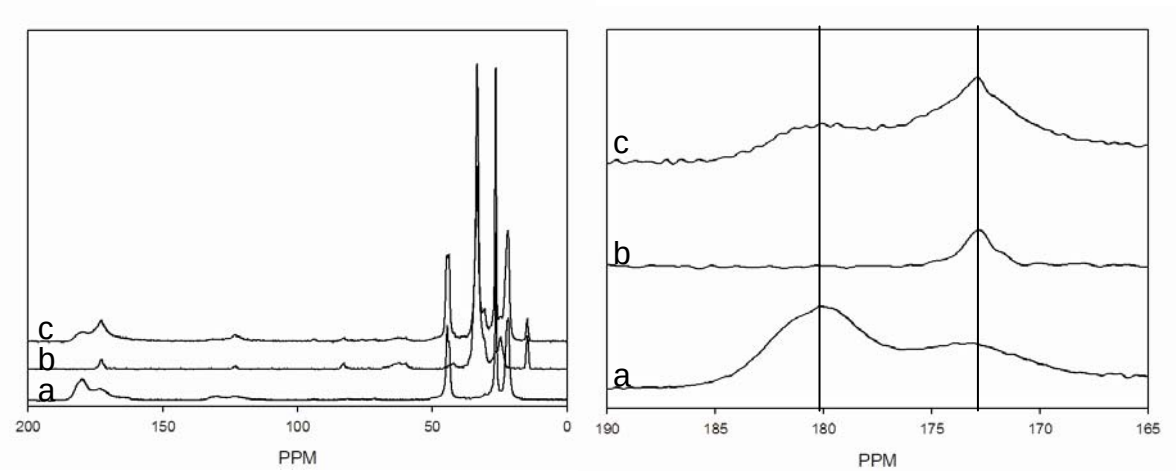

Figure 3.6 ^{13}C NMR spectra of a) MAPP; b) OP100; c) OP100/MAPP blend and an expanded view of the carbonyl region

Table 3.4 ^{13}C NMR data for OP100/MAPP blend

Chemical Shifts for OP100/MAPP blend (ppm)					**Relaxation Time ($^{H}T_{1\rho}$, ms)**			
Peaks	**MAPP**	**OP100**	**OP100/ MAPP**	**ppm change**	**MAPP**	**OP100**	**OP100/ MAPP**	**$^{H}T_{1\rho}$ change**
180	180.1±0.3		179.6±0.3		3.6±0.3A		3.1±0.7 A	
173	173.5±0.1	172.8±0.0	173.0±0.2		3.9±0.1A	4.9±0.5 A	3.6±0.4 AB	
44	44.4±0.3		44.4±0.1		5.3±0.3 B		4.6±0.3 CD	
42		42.3±0.1				2.7±0.2 B		
33		33.3±0.0	33.2±0.0	0.1ppm		3.9±0.1C	3.8±0.2ABC	
26	26.4±0.3		26.4±0.0		5.4±0.3 B		5.0±0.1 D	
24		24.7±0.0				4.1±0.2C		
21	21.9±0.3		21.9±0.1		4.9±0.1 B		4.6±0.2 CD	
14		14.6±0.0	14.6±0.0			9.1±0.5D	7.9±0.3 E	1.2ms

To further determine if any changes in chemistry occurred the $^{H}T_{1\rho}$s for each of the carbons was reviewed. While the overlap of the ester and anhydride peak does not allow for a conclusive decision as to whether there is a change or not as the two species over lap, conclusions can be drawn about the other carbons within the blend. The $^{H}T_{1\rho}$ data for this blend shows a change only in the methyl group of the OP100. The relaxation time for this peak actually decreases. This decrease in relaxation time is similar to that seen for the terminal methyl in the EBS/MAPP blend. This change indicates that there is a change in the motional

characteristics of the OP100 when crystallized in the presence of MAPP. There are no changes in $^{H}T_{1\rho}$ that show any indication of H-bonding, so while there may be some change in the motional characteristics there seems to be no significant chemical interaction between these components. Furthermore, the original phase separation seen in each component by itself is seen in the blend (denoted A,B,C). There is likely little interaction if any between the OP100 and the MAPP. This was expected as there is no effect on the MOR and MOE when OP100 is added to a MAPP containing WPC.

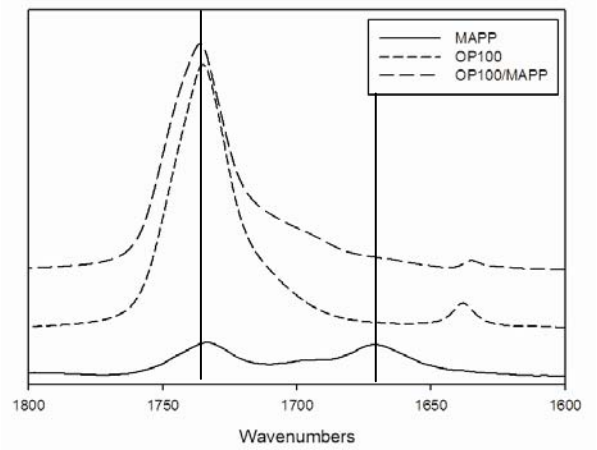

Figure 3.7 FTIR spectra expanded view of anhydride/carboxylic/ester region of MAPP, OP100 and OP100/MAPP blend

Table 3.5 FTIR band of OP100/MAPP blend (cm^{-1})

MAPP	OP100	OP100/MAPP
1733, asymmetric anhydride stretch	1735 ester stretch	1736 ester stretch
1671 symmetric anhydride stretch carboxylic acid stretch		

Again the OP100/MAPP blend was examined via IR. The resulting spectrum (Figure 3.7) shows a very large overlap between the ester region of OP100 and the anhydride/carboxylic region of the MAPP. While the overlap is significant it can be seen that there is a very small shift at the tip of the ester band from 1735cm^{-1} to 1736cm^{-1}, while the entire band has broadened towards the higher frequency side of the band by about 3cm^{-1}. This shift can be ignored as it is

below the resolution of the spectra ($4cm^{-1}$) and therefore is not significant. There is also a small broad shoulder seen at approximately $1700cm^{-1}$. This shoulder may be evidence of hydrogen bonding between the MA groups of the MAPP and the ester groups of the OP100, as hydrogen bonding shifts a band to a lower frequency. OP100 and MAPP may easily hydrogen bond due to the ester groups of OP100 and the anhydride and carboxylic groups of MAPP, therefore this band is not unexpected. No attempt to calculate the ratios between 1733/1670 or 1733/1701 was made as the overlap is far to large to accomplish this.

While no evidence of covalent interactions is seen in both the NMR and FTIR spectra, there is evidence of H-bonding between the ester functionalities of OP100 and the MA moieties of MAPP, as shown by the new and broad band at $1700cm^{-1}$ in the FTIR spectra. The mechanical properties of WPCs containing MAPP show no significant decrease when OP100 is used as a lubricant, which is consistent with these results. H-bonding would not interfere with the efficacy of MAPP to couple with wood, and therefore no decrease in mechanical properties would be expected.

3.4.4 ZnSt/MAPP

The third lubricant examined was ZnSt (Figure 3.8). Many changes are apparent in the ZnSt/MAPP blend (Figure 3.9). The most visible are the changes in chemical shift of the functional groups. First the carboxyl peak of the ZnSt at 185.3ppm shifts to 184.9ppm, the diacid peak of MAPP at 180.1ppm shifts to 181.4ppm, and the anhydride peak of MAPP at 173.5ppm to 174.4ppm, Table 3.6. The main chain peaks also experienced some change as well, the ZnSt peak at 33.9 shifted to 34.1, and the ZnSt main chain peak at 28.1 shifted to 28.5ppm, while the terminal methyl shifted to 14.7 from 14.4ppm. These shifts all indicate a significant reaction is occurring in the blend. ZnSt may cause more of the diacid of MAPP to form, or the

ZnSt may complex with the MAPP, or the stearate alone may bond with the MAPP, leaving the zinc cation to complex with the remaining carboxyl group of the MAPP.

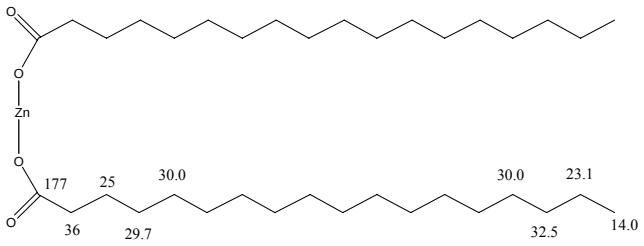

Figure 3.8 ChemDraw predictions of ^{13}C NMR spectroscopic chemical shifts for ZnSt

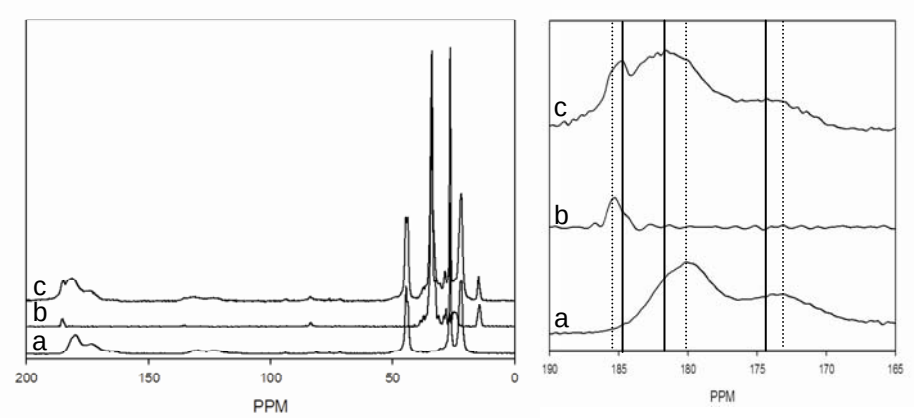

Figure 3.9 ^{13}C NMR spectra of a) MAPP; b) ZnSt; c) ZnSt/MAPP blend; and an expanded view of the carbonyl region

To determine which interactions were most likely, ChemDraw Ultra was used to create chemical predictions. Figure 3.10 shows the ZnSt and the stearate complexation reactions with MAPP, which could cause the changes seen in chemical shift of the functional groups. One possible interaction is that in which the Zn^{2+} ion is "free" and the stearate forms an anhydride bond with one of the carboxylic groups of MAPP, and the other possibility is with the carboxylic group of MAPP bonding with Zn, which is bonded with one of the stearate groups. Both predictions show a chemical shift of similar to that seen in the actual blend, 180pm and 177ppm.

Due to limitations of the software ionic predictions were not possible, though the predictions were performed to the best of the software's ability. The differences in the chemical shifts of the main chain carbons also indicate that there is a possible change in conformation, crystallinity, or mobility which can all be brought on by the interaction between the MA and carboxylic groups on the ZnSt.

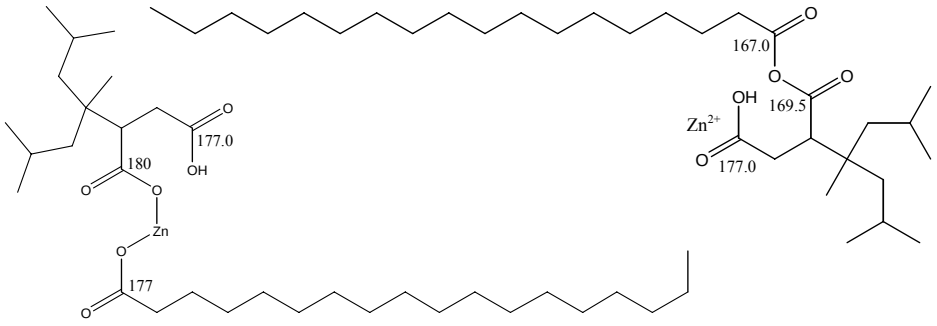

Figure 3.10 Possible chemical structures for ZnSt/MAPP interactions resulting in a chemical shift of 180ppm

Table 3.6 ^{13}C NMR data for ZnSt/MAPP blend

Chemical Shifts for ZnSt/MAPP blend (ppm)					Relaxation Time ($^{H}T_{1\rho}$, ms)			
Peaks	**MAPP**	**ZnSt**	**ZnSt/MAPP**	**ppm change**	**MAPP**	**ZnSt**	**ZnSt/MAPP**	**$^{H}T_{1\rho}$ Change**
185		185.3±0.0	184.9±0.0	0.5ppm		5.9±0.6 A	4.9±0.2, A	1.0ms
180	180.1±0.3		181.4±0.3	1.3ppm	3.6±0.3, A		3.7±0.3, B	
173	173.5±0.1		174.4±0.3	0.9ppm	3.9±0.1, A		3.5±0.3, B	
44	44.4±0.3		44.4±0.0		5.3±0.3, B		5.3±0.3, A	
33		33.9±0.0	34.1±0.0	0.2ppm		6.0±0.1 A	5.0±0.3, A	1.0ms
28		28.1±0.0	28.5±0.0	0.4ppm		5.4±0.1 A		
26	26.4±0.3		26.3±0.0		5.4±0.3, B		5.5±0.5, AC	
24		24.7±0.4				6.7±0.1 B		
21	21.9±0.3		21.9±0.0		4.9±0.1, B		4.8±0.2, A	
14		14.4±0.0	14.7±0.0	0.3ppm		9.2±0.5C	6.4±0.5, C	2.8ms

The $^{H}T_{1\rho}$ data for this blend shows no change in mobility of the MAPP carbons, while changes are noted in the ZnSt carboxylic groups, the main chain group at 33.9ppm, and the methyl group of the ZnSt, indicating it is the most changed molecule in the blend. The decrease

of 1.0ms in the $^{H}T_{1\rho}$ of carboxylic groups of ZnSt indicates that there may be H-bonding between the MAPP and the ZnSt, as seen with the decrease of the $^{H}T_{1\rho}$ of the amide peak in the EBS/MAPP blend. This change may also be due to the bonds formed between the MAPP and the ZnSt, which would change the motional characteristics of these carbons and therefore change the $^{H}T_{1\rho}$. Further evidence of a change in motional characteristics of ZnSt is the decrease of 1ms in the main chain carbons (34.1ppm) and the 2.8ms decrease in the terminal methyl carbon (14.7ppm). Interestingly both the MAPP and the ZnSt show the same phase separation after blending that was seen in the neat components, even after the changes in $^{H}T_{1\rho}$ are taken into account. Also, the carboxylic groups of the ZnSt are still phase separated from the MA moieties after blending, indicating that the zinc has a significant impact on the motional characteristics of the carboxylic groups in ZnSt. It is interesting to note that the even though the same phase separation, between the main chain carbons and the functional groups, is present, both components show similar relaxation times for their main chain carbons after blending. It seems that after blending homogeneity, and spin diffusion is present within the main chain carbons.

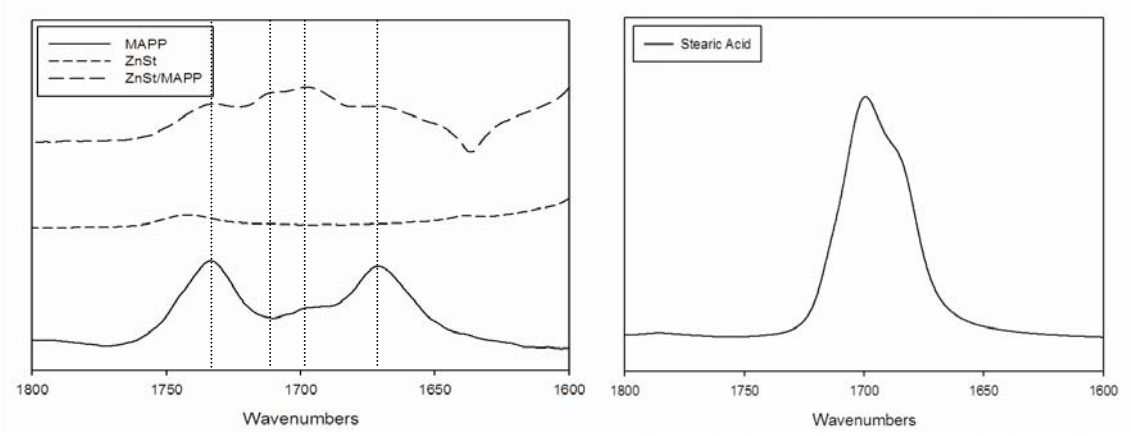

Figure 3.11 FTIR spectra: a) expanded view of anhydride region of MAPP, ZnSt and ZnSt/MAPP blend, and b) stearic acid

Table 3.7 FTIR bands and ratios* for ZnSt/MAPP blend

Band (cm^{-1})	Band Type	ZnSt/MAPP Intensity/Area	MAPP Intensity/Area
1733	asymmetric anhydride stretch	1.00	1.00
1710	ZnSt/MAPP bond	1.16(±0.09) / 0.81(±0.12)	
1697	non H-bonded carboxylic acids stearic acid	1.25(±0.09) / 1.10(±0.06)	0.52(±0.05) / 0.30(±0.04)
1670	symmetric anhydride stretch carboxylic acid stretch	0.94(±0.03) / 0.91(±0.09)	0.94(±0.01) / 0.98(±0.04)

*ratios normalized to area and intensity of $1733cm^{-1}$

Next we review the FTIR data, of which ZnSt has no overlapping bands in the anhydride region, Table 3.7. It is plainly visible in Figure 3.11 that there is a large change in chemistry occurring. The anhydride bands of MAPP have a significant decrease in intensity while there is a new and much more intense band at $1697cm^{-1}$ that appears in the blend. The new band seen at $1697cm^{-1}$ is likely due to bonding between the stearate and the MA functional groups forming and anhydride bond. Cyclic anhydrides appear at higher frequencies and therefore the anhydride formed between the stearate and the MA would no longer be cyclic and would appear at a lower frequency, as seen in Figure 3.11. Harper noted a new band a 1712 cm^{-1} and attributed this band to the formation of the diacid form of MAPP, if this were the case a band would be seen in the above spectrum around $1650cm^{-1}$. In this study a shoulder is seen at $1710cm^{-1}$, which may be from an MAPP/ZnSt bond, while the increase in intensity at $1697cm^{-1}$ appears to be due to free stearic acid. The ratios between 1671/1732 for intensity and area were determined to be 0.94 and 0.91 (Table 3.7). While the ratios of intensity and area for 1697/1732 are 1.25 and 1.10. The new band at $1710cm^{-1}$ was also examined and the ratios found to be 1.16 and 0.81 for intensity and area, respectively. From the spectrum it is plain to see that the band at $1697cm^{-1}$ is much larger in the blend than that of MAPP alone. Based on the new band at 1710 and the large increase in the band at $1697cm^{-1}$ it appears that MAPP not only bonds with the ZnSt as seen in Figure 3.10, but that it liberates stearic acid. When stearic acid is liberated the free Zn^{2+} cation

may complex with the carbonyl groups of MAPP leading to this new band at 1710cm^{-1} as well. This complexation of the Zn^{2+} cation would also inhibit the ability for MAPP to bond with wood in a ternary blend.

The downfield shifts seen in the ^{13}C NMR spectra and the appearance of a new band in the FTIR spectra are clear indications of a large chemical interaction between MAPP and ZnSt. The spectra of MAPP and Zn also shows a clear indication that zinc alone is not complexing with MAPP to cause the changes in the spectra that are seen. The downfield shift of the peaks at 180ppm and 173.5ppm seen in the ZnSt/MAPP indicate that covalent bonding between the stearate of the ZnSt and the MAPP, or between Zn, stearate, and MAPP is probably occurring. Liberation of stearic acid in the ZnSt/MAPP blend is apparent, and may lead to the complexation of the Zn^{2+} cation with the carbonyl groups of MAPP. Also, the changes in $^{H}T_{1\rho}$ of the carboxylic group of the ZnSt indicate that the motional characteristics are changing which could be due to both hydrogen bonding and to covalent bonding between the MAPP and the stearate. Further evidence of secondary interactions between the ZnSt and the MAPP can be seen by the decreases the $^{H}T_{1\rho}$ of the main chain carbons (34.1ppm) and the terminal carbon of ZnSt (14.7ppm). The FTIR spectroscopic data also shows the formation of new bonds in the presence of two new bands. The band at 1697cm^{-1}, indicates the possible presence of a new form of anhydride between the MAPP and the ZnSt. The presence of new bonds between MAPP and ZnSt is consistent with the current hypothesis that ZnSt interacts with MAPP, thus decreasing its efficacy.

3.4.5 Binary blend summary

As expected no significant interactions between EBS, OP100 and MAPP are noted. On the other hand, ZnSt blend showed significant changes in the chemistry indicating a large chemical interaction between the MAPP and ZnSt. Clearly ZnSt chemically interacts with MAPP. This is consistent with the fact that EBS and OP100 do not inhibit MAPP while ZnSt seriously decreases the efficiency of MAPP.

3.5 Ternary blends

The large interactions of ZnSt with the MAPP warranted the study of ternary blends of ZnSt/MAPP and cellulose, lignin, and maple. Namely, ZnSt/cellulose/MAPP, ZnSt/lignin/MAPP and ZnSt/maple/MAPP blends, processed at a 1:1:1 ratio.

3.5.1 ZnSt/Cellulose/MAPP

Figure 3.12 shows the spectrum of the cellulose based ternary blend. Initially one can see that there is a definite change in peak shape in the MA group region, and that the peak shapes resembles that seen in the ZnSt/MAPP more so than that seen in the cellulose/MAPP blend. The changes in chemical shift are examined, Table 3.8. The chemical shift changes seen are very similar to those seen with ZnSt/MAPP alone. The functional groups for both MAPP and ZnSt show significant increases in chemical shift, as do the chemical shifts for the C2, C3, and C5 carbons (75ppm), and the main chain carbons for the MAPP and ZnSt. The overall changes seen lead to the possible conclusion that ZnSt is reacting with the MAPP and to some extent the cellulose. This interaction would hinder the ability for MAPP to couple with the cellulose, leading to a decrease in mechanical properties, which is seen in practice.

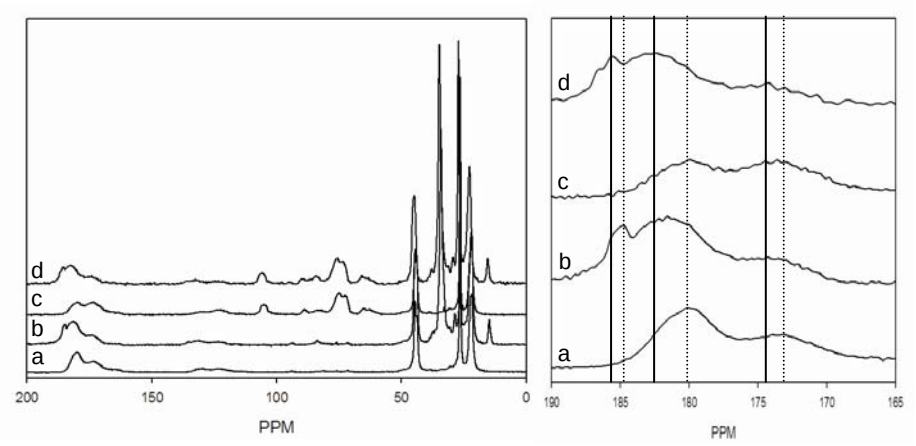

Figure 3.12 ^{13}C NMR spectra of a) MAPP; b) ZnSt/MAPP; c) Cellulose/MAPP (Chapter 2); d) ZnSt/Cellulose/MAPP (ZCM); and close up of carbonyl region

Table 3.8 ^{13}C NMR data for ZnSt/Cellulose/MAPP (ZCM) blend

Chemical Shifts for ZnSt/Cellulose/MAPP blend (ppm)						**Relaxation Time ($^{H}T_{1\rho}$, ms)**				
Peaks	**MAPP***	**ZnSt**	**Cellulose***	**ZCM**	**Change**	**MAPP***	**ZnSt**	**Cellulose***	**ZCM**	**Change**
185		185.3±0.0		185.6±0.1	0.3ppm		5.9±0.6A		5.4±0.4A	
180	180.1±0.3			182.3±0.3	1.2ppm	3.6±0.3A			4.0±0.3B	
173	173.5±0.1			174.5±0.5	1.0ppm	3.9±0.1A			4.1±0.8B	
105			105.6±0.1	105.9±0.2				5.5±0.4A	5.1±0.2A	
89			89.0±0.2	89.9±0.3				6.4±0.9A		
83			83.4±0.9	84.3±0.0				5.3±0.4A	5.3±0.3A	
74			74.9±0.1	75.8±0.1	0.9ppm			5.0±0.5A	4.3±0.2B	0.7ms
65			65.0±0.0	65.8±0.0	0.8ppm			5.6±0.7A	4.9±0.5A	
44	44.4±0.3			44.8±0.0		5.3±0.3B			5.0±0.1A	
33		33.9±0.0		34.7±0.0	0.8ppm		6.0±0.1A		5.4±0.1A	0.6ms
28		28.1±0.0		29.3±0.0	1.2ppm		5.4±0.1A		3.7±0.2B	1.7ms
26	26.4±0.3			27.1±0.0	0.7ppm	5.4±0.3B			5.8±0.1A	
24		24.7±0.4					6.7±0.1B			
21	21.9±0.3			22.7±0.0	0.8ppm	4.9±0.1B			4.8±0.1A	
14		14.4±0.0		15.4±0.0	1.0ppm		9.2±0.5C		8.0±0.3C	1.2ms

*Chapter 2

The $^{H}T_{1\rho}$ data shows that the MA groups are phase separated from the cellulose and the ZnSt, much different that what was seen in the MAPP/cellulose blend. This supports the earlier possibility that ZnSt does in fact inhibit the interaction of MAPP with wood, thereby reducing the effectiveness of MAPP. The appearance of similar relaxation times between the cellulose and the main chain of the polymers is likely due to nothing more than coincidence, rather than actual homogeneity between the polymer main chains and the cellulose as there is almost no change in the relaxation times. Based on the similarities between the ZnSt/MAPP interactions

and this ternary blend it can be concluded that when both ZnSt and cellulose are present with MAPP, the interaction between ZnSt and MAPP over powers that between MAPP and cellulose. In other words, ZnSt dominates over cellulose in interacting with MAPP.

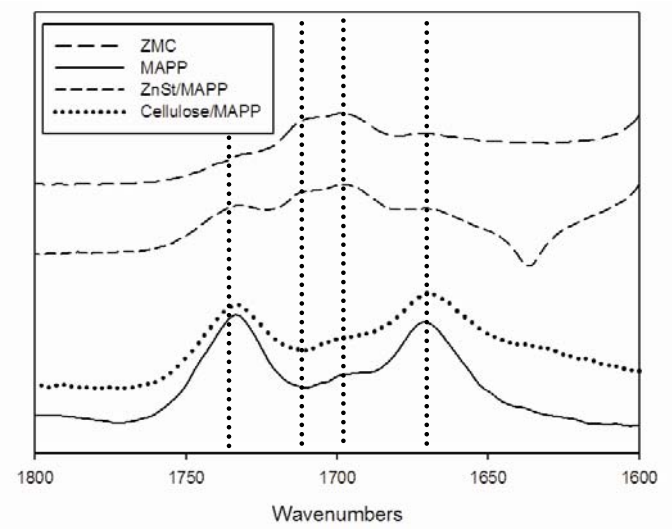

Figure 3.13 FTIR Expanded view of anhydride region of MAPP, ZnSt/MAPP, Cellulose/MAPP and ZnSt/Cellulose/MAPP (ZCM)

Table 3.9 FTIR bands of ZnSt/Cellulose/MAPP (ZCM) blend

Band (cm^{-1})	Band Type	ZCM/MAPP Intensity/Area	MAPP Intensity/Area
1732	asymmetric anhydride stretch	1.00	1.00
	ZnSt/MAPP bond		
1709	ZnSt/MAPP bond	1.92(±0.30) / 1.20(±0.35)	
1698	non H-bonded carboxylic acids stearic acid	2.16(±0.33) / 1.80(±0.42)	0.52(±0.05) / 0.30(±0.04)
1669	symmetric anhydride stretch carboxylic acid stretch	1.78(±0.45) / 2.28(±1.02)	0.94(±0.01) / 0.98(±0.04)

*ratios normalized to area and intensity of 1733cm^{-1}

Reviewing the FTIR spectroscopic data it is apparent that this blend again further resembles that of the ZnSt/MAPP blend rather than that of the Cellulose/MAPP blend (Figure 3.13). With cellulose and MAPP alone there are signs of esterification (chapter 2), whereas the ZnSt/MAPP blend shows signs of a anhydride being created between the MAPP and the ZnSt. The ternary blend also shows evidence of an anhydride between the ZnSt, and no evidence of

esterification with the cellulose. Table 3.9 lists the bands and the ratios for each of the bands. A new band is present at 1709 cm^{-1} and as with the ZnSt/MAPP blend it is likely due from bonding between the MAPP and the ZnSt or complexation of the Zn cation with the carbonyl groups of MAPP. The band at 1700cm^{-1} is much more intense than seen in MAPP alone, and the ratios of the bands show this as well. This most likely due to liberation of free stearic acid, as seen in the ZnSt/MAPP blend. If the reaction between cellulose and MAPP were to be favored, the resulting FTIR spectrum would be expected to resemble that of the MAPP/Cellulose blend. This is not the case, the ZnSt/MAPP reaction is favored instead. This is consistent with both the results of the NMR spectroscopy study as well as the prevailing literature describing the decrease in mechanical properties seen in blends containing MAPP and ZnSt (Wolcott, 2000)

3.5.2 ZnSt/Lignin/MAPP

In the ZnSt/Lignin/MAPP blend the 173ppm shows an increase in intensity while the peak at 180ppm decreases (Figure 3.14), although the peak at 180ppm is still higher in intensity than the peak at 173ppm. This behavior, again, resembles that of the ZnSt/MAPP much more than the lignin/MAPP blend. Both the MA peaks show downfield shifts, while the ZnSt peak at 185ppm does not change, Table 3.10. The chemical predictions between MAPP and ZnSt discussed previously support the possibility that the ZnSt is reacting with the MAPP. This reaction would hinder the ability of the MAPP to bond with the ZnSt. The methoxy peak of lignin also shows an increase in chemical shift as do the main chain ZnSt peak at 28ppm and the terminal methyl at 14ppm. These changes again indicate the interaction between ZnSt and MAPP is favored over any interaction between MAPP and lignin. The difference seen in the

methoxy peak is due to some chemical interaction between the lignin and the ZnSt, not the MAPP and the lignin, as no change was seen in this peak in our previous work (Chapter 2).

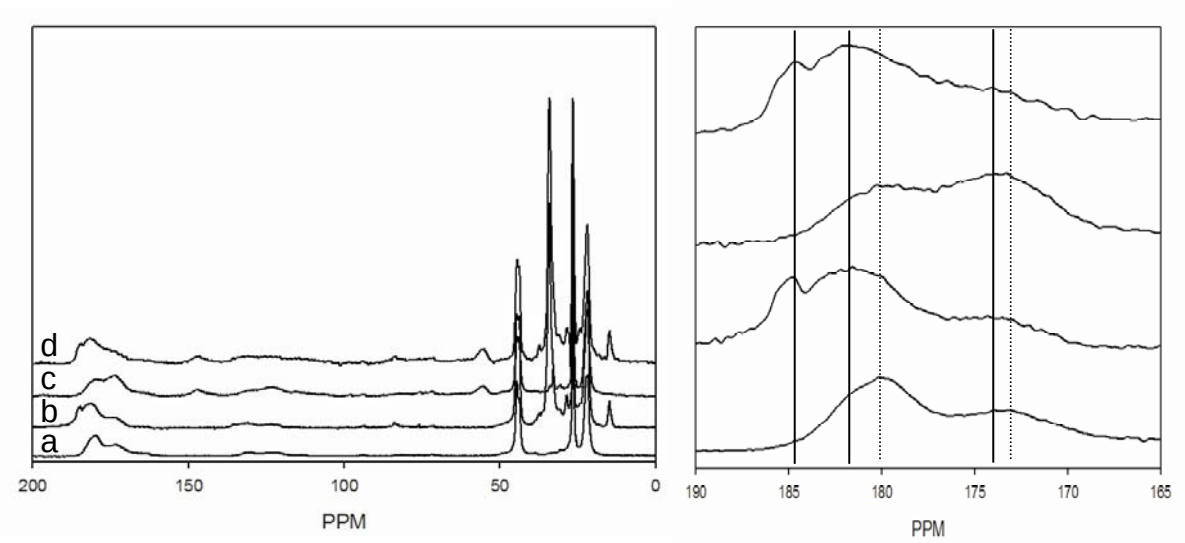

Figure 3.14 ^{13}C NMR spectra of a) MAPP; b) ZnSt/MAPP; c) Lignin/MAPP (Chapter 2); d) ZnSt/Lignin/MAPP (ZLM); and close up of carbonyl region

Table 3.10 ^{13}C NMR data for ZnSt/Lignin/MAPP blend

Chemical Shifts for ZnSt/Lignin/MAPP blend (ppm)						**Relaxation Time ($^{H}T_{1\rho}$, ms)**				
Peaks	**MAPP**	**ZnSt**	**Lignin***	**ZLM**	**Change**	**MAPP**	**ZnSt**	**Lignin**	**ZLM**	**Change**
185		185.3±0.0		185.1±0.4			5.9±0.6A		5.6±0.3A	
180	180.1±0.3			182.1±0.3	2.1ppm	3.6±0.3A			4.3±0.2B	1.7ms
173	173.5±0.1			175.4±1.1	1.9ppm	3.9±0.1A			3.9±0.8B	
147			147.5±0.2	147.5±0.7				12.8±0.9A	12.3±3.5C	
123			123.4±1.1	123.5±0.3				13.2±1.5A		
115			115.2±0.3	115.7±0.4				8.8±0.4B		
73			73.6±0.7	72.4±0.8				7.3±0.6B		
55			55.6±0.2	56.1±0.1	0.5ppm			7.9±0.2B	7.5±0.6D	
44	44.4±0.3			44.6±0.3		5.3±0.3B			4.9±0.0A	
33		33.9±0.0		34.5±0.4			6.0±0.1A		5.2±0.2A	0.8ms
28		28.1±0.0		28.9±0.4	0.8ppm		5.4±0.1A		3.6±0.2B	1.8ms
26	26.4±0.3			26.9±0.3		5.4±0.3B			5.3±0.3A	
24		24.7±0.4					6.7±0.1B			
21	21.9±0.3			22.3±0.4		4.9±0.1B			4.7±0.1A	
14		14.4±0.0		15.1±0.3	0.7ppm		9.2±0.5C		6.8±0.2D	2.4 ms

*Chapter 2

In order to further study the interactions the relaxation times of the carbons were examined. The change in $^{H}T_{1\rho}$ of the peak at 180ppm is likely due to a change in crystallinity after blending, as well as the bonding between the ZnSt and MAPP. The changes seen in the

main chain of the ZnSt peaks (33ppm and 28ppm) is also due to a change in the conformation of the chains and morphology of the blend. There is also little to no spin diffusion within the blend, as seen by the groupings, denoted A,B,C. The lignin is phase separated from the rest of the blend, while the main chain of the MAPP shows spin diffusion and homogeneity with the ZnSt main chain carbons at 33ppm. The MA functional groups of the MAPP have similar relaxation times indicating they are homogeneous, and are phase separated from the rest of the blend. While the main chain carbon of ZnSt located at 28ppm has a similar relaxation time to that of the MA functional groups, it is unlikely there is any homogeneity or spin diffusion between these carbons as they are very dissimilar. Based on the similarities between the ZnSt/MAPP blend it is evident that the ZnSt interacts with the MAPP and that this interaction dominates the blend.

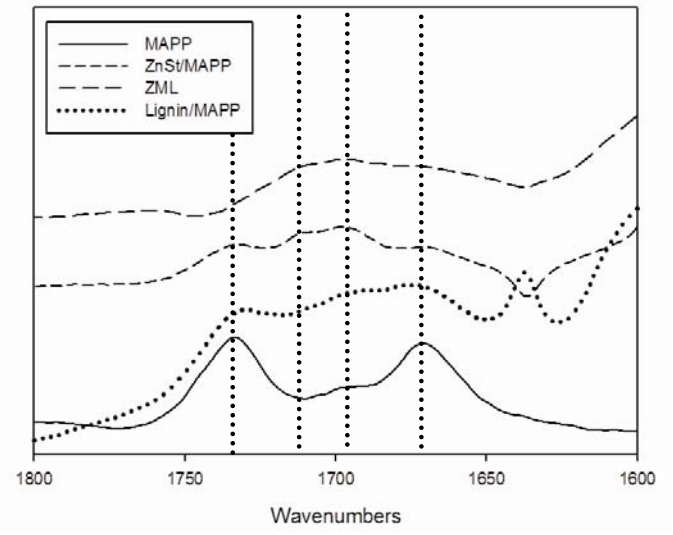

Figure 3.15 FTIR spectra: expanded view of anhydride region of MAPP, ZnSt/MAPP, ZnSt/Lignin and ZnSt/Lignin/MAPP (ZLM)

Table 3.11 FTIR bands and ratios* of ZnSt/Lignin/MAPP (ZLM) blend

Band (cm^{-1})	Band Type	ZLM/MAPP Intensity/Area	MAPP Intensity/Area
1725	asymmetric anhydride stretch	1.00	1.00
1709	ZnSt/MAPP bond	1.93(±0.13) / 1.77(±0.30)	
1697	non H-bonded carboxylic acids stearic acid	2.09(±0.12) / 2.62(±0.45)	0.52(±0.05) / 0.30(±0.04)
1670	symmetric anhydride stretch carboxylic acid stretch	0.98(±0.04) / 2.16(±0.16)	0.94(±0.01) / 0.98(±0.04)

*ratios normalized to area and intensity of $1733cm^{-1}$

A previous study has shown that a new band appears at $1637cm^{-1}$ in the lignin/MAPP blend. If the lignin/MAPP reaction were to dominate in this ternary blend, this new band would be expected. In fact, this band is not seen in the ternary blend (Figure 3.15), and there is a decrease in intensity at this particular area. The area between $1740cm^{-1}$ and $1635cm^{-1}$ in the ternary blend is very broad and no definition of the anhydride or carboxylic bands seen in the ZnSt/MAPP blend. This is partially due to overlapping lignin bands at $1740cm^{-1}$ and $1640cm^{-1}$ as well as the reaction between MAPP and ZnSt. While the bands resulting from this reaction are not fully defined the increase in intensity at $1700cm^{-1}$ indicates that the formation of both a carboxyl group as well as an anhydride between MAPP and ZnSt has occurred. It is also possible that some reaction between ZnSt and lignin may be occurring as lignin has many reactive sights that the stearate groups of ZnSt could easily react with. Table 3.11 contains the assignments for the FTIR bands and the ratios between them. There ratio between the band at 1670 and 1725 (a shoulder in this case, seems to shift but may be overlap effects) is almost 1, indicating that there could have been a chemical reaction to cause this change, or the overlap of the lignin bands may have caused it. There is a new band at $1709cm^{-1}$ and the band at $1697cm^{-1}$ has increased in intensity. These changes indicate that there is liberation of stearic acid ($1697cm^{-1}$) and that the Zn^{2+} cation may be complexing with the carbonyl groups of MAPP or MAPP may be covalently bonding with ZnSt. This As with the cellulose ternary blend, from the NMR

spectroscopic and FTIR spectroscopic data it can be surmised that the ZnSt/MAPP reaction again dominates over any other reaction. The chemical shift changes seen in the ZnSt/MAPP/Lignin blend are much more similar to that of the ZnSt/MAPP blend and point to an anhydride bond between MAPP and ZnSt and a complexation between Zn^{2+} and the carbonyl groups of MAPP rather than an ester like bond between MAPP and lignin, as do the new and broad band seen in the FTIR spectrum.

3.5.3 ZnSt/Maple/MAPP

The spectrum of the maple based ternary blend can be seen in Figure 3.16. Similar observations seen in the ZnSt/cellulose/MAPP blend and the ZnSt/lignin/MAPP blend can be made here. Namely, the ZnSt/maple/MAPP spectrum is very similar to that of the ZnSt/MAPP and different from that of the maple/MAPP blend. The changes in chemical shift are also more similar to that seen in the ZnSt/MAPP blend, Table 3.12. The diacid and anhydride chemical shifts of MAPP have a significant downfield shift. Both the C2, C3, and C5 carbons (74ppm) as well as the C1 (105ppm) characteristic carbons of cellulose show a downfield shift as well. The main chain carbons of both the MAPP and the ZnSt show the same downfield change in chemical shift as they did in the ZnSt/MAPP/cellulose blend. As with lignin the carboxyl group of the ZnSt did not show a downfield shift and this behavior is seen in the maple blend. The similarities in behavior between the ZnSt/MAPP blend, and the cellulose and lignin ternary blends appears to indicate that the ZnSt/MAPP interaction dominates the interaction of maple and MAPP.

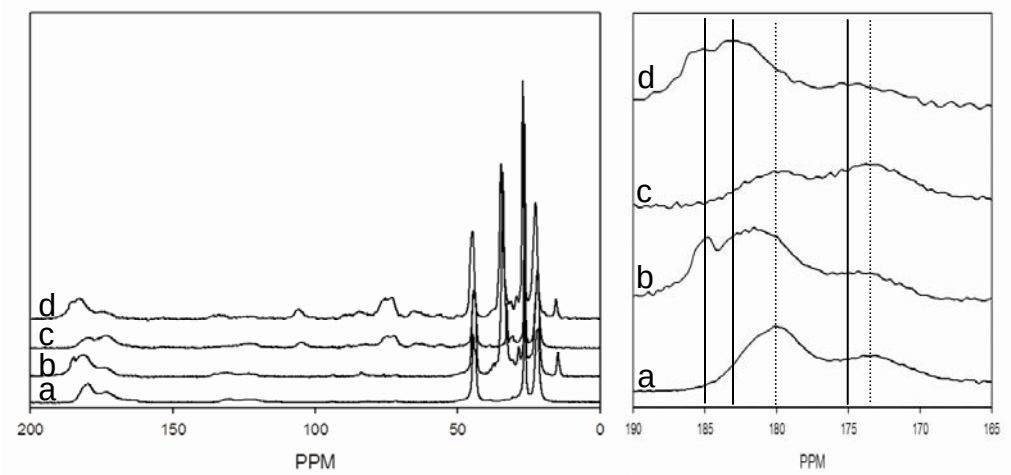

Figure 3.16 ^{13}C NMR spectra of a) MAPP; b) ZnSt/MAPP; c) Maple/MAPP (Chapter 2); d) ZnSt/Maple/MAPP (ZMM); and close up of carbonyl region

Table 3.12 ^{13}C NMR data for ZnSt/Maple/MAPP (ZMM) blend

Chemical Shifts for ZnSt/Maple/MAPP blend (ppm)						**Relaxation Time ($^{H}T_{1\rho}$, ms)**				
Peaks	**MAPP**	**ZnSt**	**Maple**	**ZMM**	**Change**	**MAPP**	**ZnSt**	**Maple**	**ZMM**	**Change**
185		185.3±0.0		185.2±0.1			5.9±0.6A		4.5±0.4A	1.4ms
180	180.1±0.3			182.9±0.2	2.8ppm	3.6±0.3A			3.7±0.1B	
173	173.5±0.1			174.9±0.5	1.5ppm	3.9±0.1A			3.9±0.5B	
105			105.4±0.1	106.0±0.1	0.6ppm			7.1±0.3A		
83			83.6±0.7	84.5±0.2				6.9±0.4A		
73			73.3±1.2	75.5±0.4	2.2ppm			6.9±0.3A	5.4±0.4C	1.5ms
64			64.4±0.9	65.5±0.2				7.3±0.9A		
55			55.6±0.6	56.4±0.3				11.1±1.2B		
44	44.4±0.3			44.8±0.0		5.3±0.3B			4.8±0.1A	
33		33.9±0.0		34.7±0.0	0.8ppm		6.0±0.1A		4.8±0.0A	1.2ms
28		28.1±0.0		29.3±0.0	1.2ppm		5.4±0.1A		3.0±0.2D	2.4ms
26	26.4±0.3			27.1±0.0	0.7ppm	5.4±0.3B			5.4±0.1C	
24		24.7±0.4					6.7±0.1B			
21	21.9±0.3			22.6±0.0	0.7ppm	4.9±0.1B			4.5±0.0A	0.4ms
20			20.4±0.2					13.0±6.0B		
14		14.4±0.0		15.4±0.0	1.0ppm		9.2±0.5C		7.1±0.6E	2.1ms

Now reviewing the relaxation data; both the MA functional groups show similar $^{H}T_{1\rho}$ after blending leading to the possibility that spin diffusion and homogeneity between these functional groups will occur. It can also be noted that these functional groups are phase separated from the carboxyl groups of the ZnSt. The change in relaxation time of the peak at 74ppm indicates that there may be some interaction between the ZnSt carboxyl groups and the hydroxyl groups of the maple as there is no evidence of interaction or homogeneity between the

maple and the MAPP, which would be expected if esterification was occurring. It appears that the MAPP has a much larger interaction with the ZnSt than the maple. Furthermore, these findings are consistent with the decreased mechanical properties found in WPCs containing both MAPP and ZnSt.

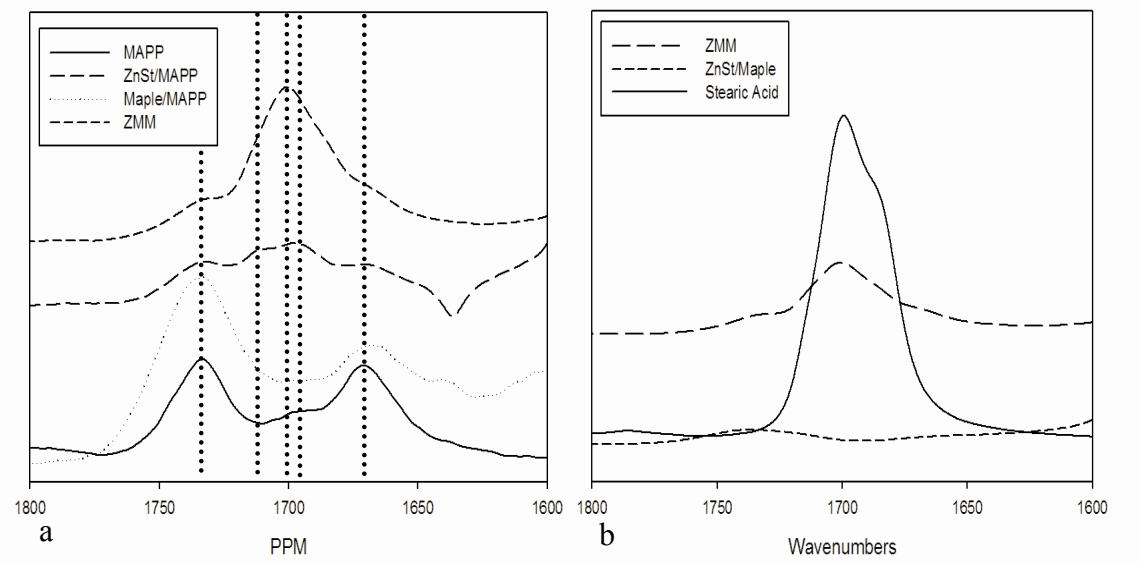

Figure 3.17 FTIR spectra: expanded view of anhydride region of a) MAPP, ZnSt/MAPP, ZnSt/Maple and ZnSt/MAPP/Maple (ZMM); b) ZnSt/Maple, Stearic acid, and ZnSt/Maple/ MAPP (ZMM)

Table 3.13 FTIR bands and ratios* of ZnSt/Maple/MAPP (ZMM) blend

Band (cm^{-1})	Band Type	ZMM/MAPP Intensity/Area	MAPP Intensity/Area
1731	asymmetric anhydride stretch	1.00	1.00
1701	non H-bonded carboxylic acids stearic acid	2.42(±0.78) / 3.27(±1.19)	0.52(±0.05) / 0.30(±0.04)
1670	symmetric anhydride stretch carboxylic acid stretch	1.06(±0.23) / 1.20(±0.19)	0.94(±0.01) / 0.98(±0.04)

*ratios normalized to area and intensity of 1733cm^{-1}

The spectrum seen in Figure 3.17 shows the FTIR data for the ZnSt/MAPP/Maple blend. It is interesting to note that there is an even larger new band seen in this blend than seen in both of the previous ternary blends. Maple has an ester peak of its own at 1735cm-1, which overlaps the asymmetrical anhydride band of the ^{13}C labeled MAPP. Not only does the anhydride band of

MAPP significantly decrease in the ternary blend, so does the ester band of the maple and a new and much more intense band appears at 1700cm^{-1}. These changes indicate that not only does the ZnSt bond with the MAPP, it also appears to react with the maple as well. To further examine the spectra the ratios of area and intensity for 1670/1731 and 1701/1731 were calculated, Table 3.13. As expected the ratio between 1701/1731 was large. The ratio for 1701/1731 was quite large and appears that more stearic acid had formed in this blend than in the other ternary blends. In order to determine if this increase was from a reaction with ZnSt and maple or a combination of all thee components a blend of ZnSt/maple was examined, Figure 3.17. There is no band at all at 1701cm^{-1} for the ZnSt/maple blend. The lack of stearic acid formation with ZnSt and maple leads to the conclusion that MAPP is a catalyst for the reaction. If ZnSt initially covalently and/or ionically bonds with MAPP the remaining stearic acid ions may abstract hydrogen from the maple thus creating more stearic acid. The Zn^{2+} cation may also ionically complex with the carbonyl groups present in maple. Maple is more acidic that both cellulose and lignin (Chapter 2) and therefore the ability for more stearic acid to form may be greater.

Maple is also known to contain hemicelluloses, O-acetyl-4-O-methylglucurono-xylan to be exact. The molar ratios of carbonyl groups was examine for ZnSt, MAPP and maple in the blend. For maple only cellulose and hemicelluloses were considered as the structure for lignin is not exact, therefore these calculations are only approximations, though the chemical composition is 41% cellulose, 25% O-acetyl-4-O-methylglucurono-xylan, and 25% lignin. Based on the 1:1:1 ratio of the blend and using the carbonyl content of ZnSt as 1 mole, it was found that there are 5.85 moles of cellulose hydroxyl groups, 0.29 moles of hemicellulose esters, 0.042 hemicellulose carboxylic acid groups, and 0.11 moles of the anhydride groups of MAPP. As maple is acidic, with a pH of 5.3 it is likely that there are several free hydrogens that may be

abstracted (Gindl and Tschegg, 2002). The large amount of carboxylic acid groups (1 mole) in the ZnSt easily explains why the new band at 1701cm^{-1} in the FTIR spectra of the ternary blend is so large. It seems that all three components are required to liberate so much of the ZnSt creating stearic acid. This may indicate that the ZnSt initially interacts with the MAPP and then may either ionically complex with the maleic anhydride moieties of the MAPP or may begin to ionically complex with the carbonyl groups in the maple. When ZnSt is blended with maple alone, the appearance of lone stearic acid is not seen, however, some evidence of lone stearic acid is seen when MAPP is blended with ZnSt. MAPP appears to be the catalyst for the liberation of stearic acid in this ternary blend. The large shifts in the NMR spectrum indicate that the reaction favored is the MAPP/ZnSt reaction and this is validated by the new band seen via FTIR spectroscopy.

3.6 Conclusions

NMR spectroscopic evaluation of the binary blends show little interaction between MAPP and EBS or OP100. Upon blending of ZnSt and MAPP, the ZnSt causes large downfield movement of the chemical shifts of the MA functional groups as well as most of the ZnSt main chain carbons. These changes are due to covalent and ionic bonding occurring between MAPP and ZnSt, and the Zn^{2+} cation during melt processing.

The further study of ternary blends containing MAPP, ZnSt and wood polymers to evaluate the full effect of ZnSt in WPCs show that the interaction of the ZnSt with the MAPP is preferred over interaction of the MAPP with the wood polymers. It was also found that with wood there appears to be a liberation of stearic acid from ZnSt, and that this reaction is catalyzed by MAPP. Overall it can be seen that ZnSt hinders the coupling between MAPP and wood by

either covalently bonding to MAPP or the Zn^{2+} cation ionically complexes with carbonyl groups of MAPP. In order to have effective coupling between MAPP and wood, the lubricants used must not be able to interact with the maleic anhydride groups of the MAPP. This means that the metal based lubricants will most likely be less effective as the metal may disassociate from the rest of the molecule leaving a metal cation or an open ended and reactive functional groups to interact and possibly hydrolyze the MAPP. An effective coupling agent will contain functional groups able to covalently bond with the hydroxyl groups of wood and in turn have a backbone compatible with the polymer matrix, such as PMPPIC.

Acknowledgements

This work was sponsored by the Office of Naval Research, under the direction of Mr. Ignacio Perez, under Grant N00014-03-1-0949.

The WSU NMR Center equipment was supported by NIH grants RR0631401 and RR12948, NSF grants CHE-9115282 and DBI-9604689 and the Murdock Charitable Trust.

3.7 References

Belfiore LA, Pieres ATN, Wang Y, Graham H, Ueda E. 1992. Transition-metal coordination in polymer blends and model systems. Macromolecules 25: 1411-1419

Gindl M, Tschegg S. 2002. Significance of the acidity of wood to the surface free energy components of different wood species. Langmuir, 18: 3209-3212.

Harper D, Wolcott M. 2004. Interaction between coupling agents and lubricants in wood-polypropylene composites. Composites Part A, 35: 385-394.

Harper DP, Wolcott MP. 2006. Chemical imagining of wood-polypropylene composites. Applied Spectroscopy, 60: 898-905.

Macomber RS. A complete introduction to modern NMR spectroscopy. 1998. New York: Wiley Interscience John Wiley & Sons, Inc.

Parker AA, Marcinko JJ, Sheih YT, Shields C, Hedrik DP, Ritchey WM. 1989. Studies of polymer morphology with ^{13}C inversion recovery cross polaization NMR. Polymer Bulletin, 21: 229-234.

Pavia DL, Lampman GM, Kriz GS. 1996. Introduction to spectroscopy: A guide for students of organic chemistry. Orlando: Harcourt Brace College Publishers.

Schmidt-Rohr K, Spiess HW. Solid state NMR and polymers. 1994. San Diego: Academic Press.

da Silva MM, Tavares MIB, Stejskal EO. 2000. ^{13}C-detected ^{1}H spin diffusion and ^{1}H relaxation study of multicomponent polymer blends. Macromolecules, 33: 115-119.

Vollhardt, K. Peter C., Neil E. Schore. 1999. Organic Chemistry: Structure and Function, Third Edition. New York : W. H. Freeman and Company.

Wolcott M, Chowdhury M, Harper D, Li T, Heath R, Rials T. 2000. Coupling Agent/Lubricant Interactions in Commercial Wood Plastic Formulations. The Sixth International Conference on Woodfiber-Plastic Composites, 197-204.

Chapter 4 General Conclusions

4.1 Summary and Conclusions

The wood plastic composite (WPC) industry has progressed significantly over the past few years, has become a larger part of the composite market and shows no signs of slowing (Deligio, 2006). The ability for this market to grow will depend in part upon the development of coupling agent/lubricant systems that allow the coupling agent to couple wood with the plastic while the lubricant allows for fast processing rates.

In this study 2 major aspects of the chemical interactions in WPCs containing the coupling agent MAPP were examined using solid state NMR spectroscopy as well as FTIR spectroscopy. First the interaction between MAPP and the wood polymers and secondly between MAPP and the lubricants were examined. Once these interactions had been identified ternary blends were evaluated to find which interactions were favored.

In this study labeled ^{13}C MAPP was used to allowed for easy determination of the characteristic peaks in the NMR spectra but also in the FTIR spectra the anhydride bands of MAPP shifted away from competing bands in the maple and lignin allowing for easier identification of chemical interactions. Evidence of esterification and hydrogen bonding was confirmed between MAPP and cellulose, lignin and maple. Chemical interactions had not previously been found between MAPP and lignin or maple due to a large overlap of the functional group bands in the FTIR spectra. This study determined that MAPP is capable of both covalent bonding; esterification; and secondary interactions; hydrogen bonding; with wood, lignin and cellulose.

Interactions between three main lubricants; ethylene bisstearamide; EBS; a poly ester OptiPak 100, OP100; and zinc stearate; ZnSt; with MAPP were then examined. No reduction of

the mechanical properties of WPCs containing MAPP and OP100 have been noted, while significant reductions in the mechanical properties of composites containing MAPP and a lubricant blend of EBS/ZnSt lubricants compared with that of WPCs containing MAPP and no lubricants have been found (Wolcott, 2000). In this study no covalent bonding was seen between EBS and MAPP or between OP100 and MAPP, while hydrogen bonding was found between the amide of EBS and MA moieties of MAPP and between the ester functionalities of OP100 and MA moieties of MAPP. Zinc Stearate (ZnSt) has long been suspected of interacting with MAPP thus reducing its efficacy (Harper 2004, 2006; Wolcott, 2000). Anhydride bonds were found to have formed between the ZnSt and the MAPP, leaving a remaining carboxylic acid group. Also, it was determined that the Zn^{2+} cation can complex with the carbonyl groups of MAPP thus inhibiting its efficacy, as well liberating stearic acid. As this reaction was the only one seen between MAPP and any of the lubricants, ternary blends containing each of the wood polymers, MAPP, and ZnSt were reviewed.

The three ternary blends containing cellulose, lignin, and maple all showed significant signs of chemical interaction. Interestingly the interactions discovered were not between MAPP and the wood polymers, as is expected when using a coupling agent, but between the MAPP and the ZnSt. Again, evidence of the ZnSt forming anhydride bonds with the MAPP leaving a remaining carboxylic acid was present. ZnSt also appeared to react with the extractives and hemicelluloses of maple as well. The efficacy of is significantly reduced when the ZnSt/MAPP interaction is favored over that of esterification with wood.

Several popular types of coupling agents include isocyanates, anhydrides, anhydride modified polyolefins, and silanes (Lu, 2000; Matías, 2000; Jana, 2002). The more functional groups present, *i.e.* maleic anhydride with two carboxylic groups, the greater the graft reactivity

(Lu, 2000). Isocyanates and silanes are capable of bonding with the hydroxyl groups of the wood surface as well. Not only is the functional group in the coupling agent important, but the polymer matrix it may be attached it is very important as well. Higher mechanical properties can be obtained if the backbones of both the polymer matrix and the coupling agent are similar. For instance, a composite with a polyethylene backbone in conjunction with maleic anhydride polyethylene has higher mechanical properties than in MAPP were used (Wang, 2003).

Further study into different lubricant/MAPP/wood polymer interactions is required to develop efficient coupling agent/lubricant systems. Based on the results of this study one can conclude that for MAPP to act as a coupling agent the lubricant used must not be a metal based lubricant. The metal is able to dissociate from the rest of the molecule allowing for competing reactions to take place. Also, the coupling agent must contain functional groups able to chemically bond with wood.

4.2 References

Deligio T. 2006. Wood-plastic composites build new markets. Modern Plastics

Harper D, Wolcott M. 2004. Interaction between coupling agents and lubricants in wood-polypropylene composites. Composites Part A, 35: 385-394.

Harper DP, Wolcott MP. 2006. Chemical imagining of wood-polypropylene composites. Applied Spectroscopy, 60: 898-905.

Jana SC, Priet A. 2002. Natural fiber composites of high-temperature thermoplastic polymers: Effects of coupling agents. Journal of Applied Polymer Science, 86: 2168-2173.

Lu JZ, Wu Q, McNabb HS Jr. 2000. Chemical coupling in wood fiber and polymer composites: a review of coupling agents and treatments. Wood and Fiber Science, 32: 88-104.

Wang Y, Yeh FC, Lai SM, Chan HC, Shen HF. 2003. Effectiveness of functionalized polyolefins as compatibilizers for polyethylene/wood flour composites. Polymer Engineering and Science, 43: 933-945.

Wolcott M, Chowdhury M, Harper D, Li T, Heath R, Rials T. 2000. Coupling agent/lubricant interactions in commercial wood plastic formulations. The Sixth International Conference on Woodfiber-Plastic Composites, 197-204.

APPENDIX

A Raw NMR Peak Data

Table A.1 MAPP (ppm)

1	2	3	Average	Stdev
179.8	180.2	180.5	180.1	0.3
173.5	173.5	173.6	173.5	0.1
165.2	166.0	166.1	165.8	0.5
44.1	44.6	44.6	44.4	0.3
26.0	26.6	26.6	26.4	0.3
21.5	22.1	22.0	21.9	0.3

Table A.2 Cellulose (ppm)

1	2	3	Average	Stdev
105.6	105.4	105.6	105.5	0.1
88.8	89.1	89.1	89.0	0.2
82.6	84.3	83.1	83.4	0.9
75.0	74.9	74.7	74.9	0.1
65.0	65.1	65.0	65.0	0.0

Table A.3 Lignin (ppm)

1	2	3	Average	Stdev
147.8	147.3	147.5	147.5	0.2
122.7	124.7	122.8	123.4	1.1
115.4	115.3	114.8	115.2	0.3
73.6	73.0	74.3	73.6	0.7
55.6	55.4	55.2	55.4	0.2
35.7	36.3	33.8	35.2	1.3

Table A.4 Maple (ppm)

1	2	3	Average	Stdev
105.2	105.5	105.4	105.4	0.1
83.2	83.2	84.4	83.6	0.7
74.6	72.8	72.4	73.3	1.2
64.7	63.4	65.2	64.4	0.9
56.1	55.8	54.9	55.6	0.6
20.3	20.6	20.2	20.4	0.2

Table A.5 EBS (ppm)

1	2	3	Average	Stdev
173.6	173.6	173.6	173.6	0.0
40.2	40.2	40.3	40.2	0.0
33.9	33.9	33.9	33.9	0.0
27.0	27.0	27.0	27.0	0.0
24.6	24.6	24.6	24.6	0.0
14.3	14.3	14.3	14.3	0.0

Table A.6 OP100 (ppm)

1	2	3	Average	Stdev
172.8	172.8	172.8	172.8	0.0
82.9	82.9	82.9	82.9	0.0
62.1	62.5	62.2	62.3	0.2
42.4	42.2	42.3	42.3	0.1
33.3	33.3	33.3	33.3	0.0
24.7	24.7	24.7	24.7	0.0
14.6	14.6	14.6	14.6	0.0

Table A.7 ZnSt (ppm)

1	2	3	Average	Stdev
185.3	185.3	185.3	185.3	0.0
33.9	33.9	33.9	33.9	0.0
28.1	28.1	28.1	28.1	0.0
24.9	24.9	24.3	24.7	0.4
14.4	14.4	14.4	14.4	0.0

Table A.8 Cellulose/MAPP (ppm)

1	2	3	Average	Stdev
179.6	180.0	180.4	180.0	0.4
173.2	173.2	173.8	173.4	0.3
104.9	105.4	105.6	105.3	0.4
88.7	89.4	89.7	89.3	0.5
82.3	83.4	82.3	82.7	0.6
74.7	74.8	74.9	74.8	0.1
64.8	65.2	65.4	65.1	0.3
44.0	43.9	44.4	44.1	0.3
32.4	32.6	32.7	32.6	0.2
26.0	26.4	26.4	26.2	0.2
21.5	21.9	21.9	21.8	0.2

Table A.9 Lignin/MAPP (ppm)

1	2	3	Average	Stdev
179.3	180.1	179.3	**179.6**	**0.4**
173.5	174.2	174.0	**173.9**	**0.4**
146.8	148.0	146.9	**147.2**	**0.6**
123.6	124.5	123.2	**123.8**	**0.7**
115.0	116.9	115.8	**115.9**	**1.0**
55.4	55.2	55.7	**55.4**	**0.2**
44.0	44.4	44.3	**44.3**	**0.2**
32.4	32.8	32.8	**32.7**	**0.2**
26.0	26.4	26.5	**26.3**	**0.3**
21.4	21.9	21.9	**21.8**	**0.3**

Table A.10 Maple/MAPP (ppm)

1	2	3	Average	Stdev
179.8	180.1	179.6	179.8	0.2
173.4	173.2	173.7	173.4	0.2
104.9	104.8	105.5	105.1	0.4
82.0	82.6	82.8	82.5	0.4
74.3	75.0	74.8	74.7	0.4
64.8	65.9	65.0	65.3	0.6
56.1	56.7	56.5	56.4	0.3
44.0	44.4	44.4	44.3	0.2
32.3	32.7	32.8	32.6	0.2
26.0	26.4	26.4	26.3	0.2
21.5	21.9	21.9	21.8	0.3

Table A.11 EBS/MAPP (ppm)

1	2	3	Average	Stdev
179.9	180.5	179.6	180.0	0.5
173.5	173.7	173.7	173.7	0.1
44.4	44.4	44.4	44.4	0.0
40.1	40.3	40.3	40.2	0.1
34.0	34.0	34.0	34.0	0.0
26.3	26.4	26.4	26.4	0.0
21.9	21.9	21.9	21.9	0.0
14.4	14.2	14.4	14.3	0.1

Table A.12 OP100/MAPP (ppm)

1	2	3	Average	Stdev
179.3	179.9	179.8	179.6	0.3
172.8	173.2	172.9	173.0	0.2
44.3	44.5	44.4	44.4	0.1
33.3	33.3	33.2	33.2	0.0
26.4	26.4	26.4	26.4	0.0
21.8	21.9	21.8	21.9	0.1
14.7	14.6	14.6	14.6	0.0

Table A.13 ZnSt/MAPP (ppm)

1	2	3	Average	Stdev
184.9	184.8	184.9	184.9	0.0
181.6	181.6	181.1	181.4	0.3
174.3	174.1	174.7	174.4	0.3
44.4	44.4	44.4	44.4	0.0
34.1	34.0	34.1	34.1	0.0
28.5	28.6	28.5	28.5	0.0
26.4	26.3	26.3	26.3	0.0
21.9	21.9	21.9	21.9	0.0
14.7	14.7	14.7	14.7	0.0

Table A.14 ZnSt/Cellulose/MAPP (ppm)

1	2	3	Average	Stdev
185.6	185.6	185.4	185.6	0.1
182.5	182.5	182.0	182.3	0.3
174.3	175.0	174.2	174.5	0.5
105.9	105.6	106.1	105.9	0.2
90.0	90.0	89.5	89.9	0.3
84.3	84.4	84.3	84.3	0.0
75.7	75.9	75.9	75.8	0.1
65.8	65.9	65.8	65.8	0.0
44.9	44.9	44.8	44.8	0.0
34.7	34.7	34.7	34.7	0.0
29.3	29.3	29.3	29.3	0.0
27.1	27.1	27.1	27.1	0.0
22.7	22.7	22.7	22.7	0.0
15.4	15.3	15.4	15.4	0.0

Table A.15 ZnSt/Lignin/MAPP (ppm)

1	2	3	Average	Stdev
184.6	185.3	185.4	185.1	0.4
181.8	182.4	182.1	182.1	0.3
174.1	175.7	176.3	175.4	1.1
146.8	147.5	148.2	147.5	0.7
123.7	123.6	123.2	123.5	0.3
115.9	115.8	115.3	115.7	0.4
71.5	72.6	73.1	72.4	0.8
55.9	56.1	56.1	56.1	0.1
44.3	44.8	44.8	44.6	0.3
34.0	34.7	34.7	34.5	0.4
28.4	29.1	29.1	28.9	0.4
26.5	27.0	27.0	26.9	0.3
21.9	22.6	22.6	22.3	0.4
14.8	15.3	15.3	15.1	0.3

Table A.16 ZnSt/Maple/MAPP (ppm)

1	2	3	Average	Stdev
185.1	185.1	185.3	185.2	0.1
183.0	183.1	182.8	182.9	0.2
175.5	174.6	174.5	174.9	0.5
105.9	106.1	105.9	106.0	0.1
84.7	84.4	84.6	84.5	0.2
75.6	75.8	75.0	75.5	0.4
65.4	65.7	65.4	65.5	0.2
56.6	56.5	56.0	56.4	0.3
44.8	44.8	44.7	44.8	0.0
34.8	34.7	34.7	34.7	0.0
29.3	29.3	29.2	29.3	0.0
27.1	27.1	27.1	27.1	0.0
22.6	22.6	22.6	22.6	0.0
15.4	15.4	15.4	15.4	0.0

B Raw NMR $^{H}T_{1\rho}$ Data

Table B.1 MAPP (ms)

Peaks	1	2	3	Average	StDev
180.1	3.2	3.8	3.8	3.6	0.3
173.8	3.9	3.8	3.9	3.9	0.1
44.5	4.9	5.3	5.6	5.3	0.3
26.8	5.0	5.4	5.7	5.4	0.3
21.8	4.9	4.9	5.0	4.9	0.1

Table B.2 Cellulose (ms)

Peaks	1	2	3	Average	Stdev
105.6	5.1	5.5	5.8	5.5	0.4
88.8	6.5	5.4	7.2	6.4	0.9
82.6	5.1	5.0	5.7	5.3	0.4
75.0	4.5	5.1	5.4	5.0	0.5
65.0	4.8	6.1	5.9	5.6	0.7

Table B.3 Lignin (ms)

Peaks	1	2	3	Average	Stdev
147.8	12.1	13.9	12.5	12.8	0.9
122.7	12.1	12.6	14.9	13.2	1.5
115.4	8.4	8.90	9.10	8.8	0.4
73.6	6.60	7.7	7.7	7.3	0.6
55.6	7.8	8.1	7.9	7.9	0.2
35.7	6.80	7.00	8.5	7.4	0.9

Table B.4 Maple (ms)

Peaks	1	2	3	Average	Stdev
105.2	6.9	7.5	6.9	7.1	0.3
83.2	7.3	6.6	6.7	6.9	0.4
72.4	7.2	6.6	6.8	6.9	0.3
64.7	6.7	6.8	8.3	7.3	0.9
56.1	12.5	10.2	10.7	11.1	1.2
20.3	8.8	19.9	10.3	13.0	6.0

Table B.5 EBS (ms)

Peaks	1	2	3	Average	Stdev
173.0	4.9	4.7	4.6	4.7	0.2
40.0	4.8	4.8	4.9	4.8	0.1
33.9	5.4	5.4	5.4	5.4	0.0
27.0	4.7	5.0	4.9	4.9	0.2
24.7	5.3	5.5	5.3	5.4	0.1
14.0	6.4	6.2	6.8	6.5	0.3

Table B.6 OP100 (ms)

Peaks	1	2	3	Average	Stdev
172.6	4.3	5.2	5.2	4.9	0.5
83.6	2.8	3.1	2.7	2.9	0.2
62.4	2.9	3.0	2.8	2.9	0.1
42.4	2.6	2.7	2.9	2.7	0.2
33.3	3.8	4.0	4.0	3.9	0.1
24.8	3.9	4.1	4.2	4.1	0.2
14.7	8.6	9.1	9.5	9.1	0.5

Table B.7 ZnSt (ms)

ZnSt	1	2	3	Average	Stdev
185.3	5.7	5.5	6.6	5.9	0.6
33.9	6.1	6.0	6.0	6.0	0.1
28.1	5.4	5.5	5.4	5.4	0.1
24.9	6.7	6.7	6.8	6.7	0.1
14.4	9.7	8.8	9.0	9.2	0.5

Table B.8 Cellulose/MAPP (ms)

Peaks	1	2	3	Average	StDev
180.1	3.3	4.1	3.6	3.6	0.4
173.5	3.7	3.9	4.3	3.9	0.3
44.0	4.5	4.5	4.8	4.6	0.2
104.0	3.4	4.9	4.7	4.3	0.8
74.7	3.2	4.1	4.5	4.0	0.7
32.4	2.6	2.4	3.0	2.6	0.3
26.8	4.9	5.2	5.2	5.1	0.2
21.8	4.1	4.5	4.4	4.3	0.2

Table B.9 Lignin/MAPP (ms)

Peaks	1	2	3	Average	Stdev
180.1	3.2	5.1	4.0	4.1	1.0
173.5	4.5	5.5	5.2	5.0	0.5
44.0	4.8	5.4	5.0	5.1	0.3
54.9	6.5	6.5	6.1	6.4	0.2
32.4	2.8	4.4	3.4	3.5	0.8
26.8	5.3	5.5	5.6	5.5	0.2
21.8	4.4	5.0	4.9	4.8	0.3

Table B.10 Maple/MAPP (ms)

Peaks	1	2	3	Average	Stdev
180.1	2.7	3.4	3.1	3.1	0.3
173.5	3.3	3.5	3.7	3.5	0.2
44.5	4.2	4.6	4.3	4.3	0.2
104.5	4.0	4.6	4.3	4.3	0.3
74.5	3.7	4.0	4.7	4.1	0.5
32.4	3.3	4.0	4.2	3.8	0.5
26.8	4.7	5.2	5.2	5.0	0.3
21.8	4.0	4.6	4.4	4.3	0.3

Table B.11 EBS/MAPP (ms)

Peaks	1	2	3	Average	StDev
180.1	3.3	4.0	3.9	3.7	0.4
173.8	3.5	3.8	4.1	3.8	0.3
44.5	5.0	5.1	5.3	5.1	0.2
40	3.7	4.5	4.0	4.0	0.4
33.9	4.5	5.3	5.5	5.1	0.5
26.8	5.4	5.9	5.3	5.5	0.3
21.8	4.8	5.2	5.1	5.0	0.2
14.2	4.7	5.1	5.2	5.0	0.3

Table B.12 OP100/MAPP (ms)

Peaks	1	2	3	Average	Stdev
180.1	2.4	3.1	3.7	3.1	0.7
173.8	3.4	3.3	4.1	3.6	0.4
44.5	4.3	5.0	4.6	4.6	0.3
33.3	3.6	3.7	3.9	3.8	0.2
26.8	4.9	4.8	5.1	5.0	0.1
21.7	4.3	4.7	4.7	4.6	0.2
14.7	7.6	8.2	8.0	7.9	0.3

Table B.13 ZnSt/MAPP (ms)

Peaks	1	2	3	Average	Stdev
180.1	3.4	3.9	3.7	3.7	0.3
173.8	3.3	3.3	3.8	3.5	0.3
44.5	5.0	5.7	5.4	5.3	0.3
185	4.9	4.7	5.0	4.9	0.2
34.1	4.7	5.3	5.2	5.0	0.3
26.4	4.9	5.9	5.6	5.5	0.5
21.8	4.5	5.0	4.9	4.8	0.2
14.7	6.3	6.9	5.9	6.4	0.5

Table B.14 ZnSt/Cellulose/MAPP (ms)

Peaks	1	2	3	Average	Stdev
185.4	5.5	5	5.7	5.4	0.4
182.0	3.7	3.9	4.3	4.0	0.3
174.2	3.2	4.7	4.5	4.1	0.8
106.1	5.2	4.9	5.2	5.1	0.2
84.3	5.1	5.1	5.6	5.3	0.3
75.9	4.2	4.1	4.4	4.2	0.2
65.8	5.4	4.4	5	4.9	0.5
44.8	5	4.9	5.1	5.0	0.1
34.7	5.4	5.4	5.5	5.4	0.1
29.3	3.8	3.5	3.7	3.7	0.2
27.1	5.7	5.9	5.8	5.8	0.1
22.7	4.7	4.9	4.9	4.8	0.1
15.4	8	8.3	7.7	8.0	0.3

Table B.15 ZnSt/Lignin/MAPP (ms)

Peaks	1	2	3	Average	Stdev
185.4	5.3	5.8	5.6	5.6	0.3
182.1	4.3	4.2	4.5	4.3	0.2
176.3	4.8	3.5	3.3	3.9	0.8
148.2	16.3	10.8	9.8	12.3	3.5
56.1	7.4	6.9	8.1	7.5	0.6
44.8	4.9	4.9	4.9	4.9	0.0
34.7	5.4	5	5.1	5.2	0.2
29.1	3.8	3.6	3.5	3.6	0.2
27.0	5	5.4	5.5	5.3	0.3
22.6	4.8	4.7	4.7	4.7	0.1
15.3	6.9	6.8	6.6	6.8	0.2

Table B.16 ZnSt/Maple/MAPP (ms)

Peaks	1	2	3	Average	Stdev
185.3	4.1	4.8	4.5	4.5	0.4
182.8	3.7	3.6	3.7	3.7	0.1
174.5	4.3	4.1	3.4	3.9	0.5
75.0	5	5.8	5.3	5.4	0.4
44.7	4.8	4.9	4.8	4.8	0.1
34.7	4.8	4.8	4.8	4.8	0.0
29.2	2.8	3.2	3	3.0	0.2
27.1	5.5	5.3	5.3	5.4	0.1
22.6	4.5	4.5	4.5	4.5	0.0
15.4	7.2	6.5	7.6	7.1	0.6

C Raw FTIR Spectroscopy Data

Table C.1 MAPP (cm^{-1})

1	2	3	Average
1801	1797	1798	**1799**
1733	1733	1733	**1733**
1671	1671	1671	**1671**

Table C.2 Cellulose (cm^{-1})

1	2	3	Average
1635	1643	1638	**1639**

Table C.3 Lignin (cm^{-1})

1	2	3	Average
1695	1693	1694	**1694**
1594	1594	1594	**1594**

Table C.4 Maple (cm^{-1})

1	2	3	Average
1735	1735	1735	**1735**
1657	1657	1656	**1657**
1593	1593	1593	**1593**

Table C.5 EBS (cm^{-1})

1	2	3	Average
1637	1637	1637	**1637**
1709	1708	1706	**1708**
1738	1738	1738	**1738**

Table C.6 OP100 (cm^{-1})

1	2	3	Average
1735	1735	1735	**1735**
1638	1638	1638	**1638**

Table C.7 ZnSt (cm^{-1})

1	2	3	Average
1741	1743	1742	**1742**
1739	1739	1739	**1739**

Table C.8 EBS/MAPP (cm^{-1})

1	2	3	Average
1636	1636	1635	**1636**
1733	1733	1733	**1733**
1694	1696	1696	**1695**
1670	1669	1669	**1669**

Table C.9 OP100/MAPP (cm^{-1})

1	2	3	Average
1736	1736	1737	**1736**

Table C.10 ZnSt/MAPP (cm^{-1})

1	2	3	Average
1732	1732	1731	**1732**
1711	1710	1709	**1710**
1697	1697	1697	**1697**
1671	1670	1671	**1671**

Table C.11 Cellulose/MAPP (cm^{-1})

1	2	3	Average
1733	1733	1734	**1733**
1702	1698	1694	**1698**
1670	1670	1670	**1670**

Table C.12 Lignin/MAPP (cm^{-1})

1	2	3	Average
1731	1730	1731	**1731**
1694	1695	1694	**1694**
1674	1673	1673	**1673**
1637	1637	1637	**1637**
1595	1595	1596	**1595**

Table C.13 Maple/MAPP (cm^{-1})

1	2	3	Average
1734	1734	1734	**1734**
1669	1668	1669	**1669**
1640	1640	1638	**1639**
1700	1698	1697	**1698**

Table C.14 ZnSt/Cellulose/MAPP (cm^{-1})

1	2	3	Average
1732	1731	1732	**1732**
1709	1709	1710	**1709**
1699	1697	1697	**1698**
1670	1666	1670	**1669**

Table C.15 ZnSt/Lignin/MAPP (cm^{-1})

1	2	3	Average
1723	1726	1726	**1725**
1709	1709	1709	**1709**
1698	1697	1696	**1697**

Table C.16 ZnSt/Maple/MAPP (cm^{-1})

1	2	3	Average
1731	1731	1731	**1731**
1701	1701	1700	**1701**
1670	1668	1672	**1670**